The Yamato-type (CY) carbonaceous chondrite group: Analogues for the surface of asteroid Ryugu?

Journal Item

Geochemistry xxx (xxxx) xxx–xxx

Contents lists available at ScienceDirect

Geochemistry

journal homepage: www.elsevier.com/locate/chemer

The Yamato-type (CY) carbonaceous chondrite group: Analogues for the surface of asteroid Ryugu?

A.J. King[a,*], H.C. Bates[a,b], D. Krietsch[c], H. Busemann[c], P.L. Clay[d], P.F. Schofield[a], S.S. Russell[a]

[a] Planetary Materials Group, Department of Earth Sciences, Natural History Museum, Cromwell Road, London, SW7 5BD, UK
[b] Atmospheric, Oceanic and Planetary Physics Department, Clarendon Laboratory, University of Oxford, Sherrington Road, Oxford, OX1 3P, UK
[c] Institute of Geochemistry and Petrology, ETH Zürich, Clausiusstrasse 25, 8092 Zürich, Switzerland
[d] School of Earth and Environmental Sciences, University of Manchester, Manchester, M13 9PL, UK

ARTICLE INFO

Handling Editor: Falko Langenhorst

Keywords:
Carbonaceous chondrite
Aqueous alteration
Thermal metamorphism
Asteroids
Meteorites
Ryugu
Hayabusa-2

ABSTRACT

We report new mineralogical, petrographic and noble gas analyses of the carbonaceous chondrite meteorites Y-82162 (C1/2$_{ung}$), Y-980115 (CI1), Y-86029 (CI1), Y-86720 (C2$_{ung}$), Y-86789 (C2$_{ung}$), and B-7904 (C2$_{ung}$). Combining our results with literature data we show that these meteorites experienced varying degrees of aqueous alteration followed by short-lived thermal metamorphism at temperatures of > 500 °C. These meteorites have similar mineralogy, textures and chemical characteristics suggesting that they are genetically related, and we strongly support the conclusion of Ikeda (1992) that they form a distinct group, the CYs ("Yamato-type"). The CY chondrites have the heaviest oxygen isotopic compositions ($\delta^{17}O$ ~12‰, $\delta^{18}O$ ~22‰) of any meteorite group, high abundances of Fe-sulphides (~10 – 30 vol%) and phosphates, and contain large grains of periclase and unusual objects of secondary minerals not reported in other carbonaceous chondrites. These features cannot be attributed to parent body processes alone, and indicate that the CYs had a different starting mineralogy and/or alteration history to other chondrite groups, perhaps because they formed in a different region of the protoplanetary disk. The short cosmic-ray exposure ages (≤1.3 Ma) of the CY chondrites suggest that they are derived from a near-Earth source, with recent observations by the Hayabusa2 spacecraft highlighting a possible link to the rubble-pile asteroid Ryugu.

1. Introduction

Carbonaceous chondrite meteorites are among the most pristine extraterrestrial materials available for study. They contain a mixture of chondrules, calcium-aluminium rich inclusions (CAIs) and silicate clasts set within a fine-grained (< 1 μm) matrix and are chemically primitive, with bulk elemental compositions similar to the solar photosphere (for reviews see Brearley and Jones, 1998 and Weisberg et al., 2006). Carbonaceous chondrites make up < 5% of all known meteorites and are classified into at least eight petrologic groups based on their mineralogical, elemental and isotopic properties. Variations in these properties reflect differences in the spatial and/or temporal formation and geological evolution of their asteroid parent bodies.

The phyllosilicate-rich (> 60 vol%) CI, CM, and CR carbonaceous chondrites indicate that low temperature (< 150 °C) aqueous alteration was a significant process on primitive asteroids (Zolensky et al., 1993; Brearley, 2006; Howard et al., 2015; King et al., 2015a). Studying the hydrated carbonaceous chondrite groups provides information about the nature and distribution of water and other volatile species in the early solar system (e.g. Alexander et al., 2012). There are also a number of carbonaceous chondrites that underwent extensive aqueous alteration, but do not fit into the traditional CI, CM, and CR groups. These ungrouped hydrated meteorites potentially offer new insights into the conditions on asteroids and the diversity of materials that delivered water to the terrestrial planets.

Three unusual meteorites recovered from Antarctica, Yamato (Y)-82162 (C1/2$_{ung}$), Y-86720 (C2$_{ung}$) and Belgica (B)-7904 (C2$_{ung}$), were investigated in the late 1980's by an international consortium, with the final results summarised by Ikeda (1992). Sometimes referred to as the "Belgica Grouplet", all three meteorites experienced parent body aqueous alteration, and have mineralogy, textures and elemental compositions often intermediate between the CI and CM chondrites. In addition to aqueous alteration, these three meteorites also record a late stage thermal metamorphic event(s) at peak temperatures > 500 °C that dehydrated the phyllosilicates, caused recrystallization of olivine, and melted Fe-sulphides. Furthermore, the bulk oxygen isotopic

* Corresponding author.
E-mail address: a.king@nhm.ac.uk (A.J. King).

https://doi.org/10.1016/j.chemer.2019.08.003
Received 15 May 2019; Received in revised form 13 August 2019; Accepted 19 August 2019

compositions of Y-82162, Y-86720 and B-7904 were found to be heavier than any other carbonaceous chondrite, leading Ikeda (1992) to propose that they formed a new group, the CYs ("Yamato-type"). In the last ~30 years other potential members of the CY group have been identified; Y-86789 ($C2_{ung}$) is likely paired with Y-86720 (Matsuoka et al., 1996), and Y-86029 and Y-980115, although officially classified as CI chondrites, have very similar mineralogical and chemical characteristics to Y-82162 (Tonui et al., 2014; King et al., 2015a). However, the CY nomenclature has never been widely adopted by the community.

The petrologic classification of carbonaceous chondrites is a crucial step towards understanding the complex processes that formed and modified the first planetesimals. Here, we combine new mineralogical, petrographic and noble gas analyses with literature results to revisit the major characteristics of the CY meteorites and outline the evidence for them forming a distinct chondrite group. This effort is timely as aqueously altered and thermally metamorphosed meteorites appear to be the closest spectral match to materials on the surface of asteroid Ryugu, from which the Hayabusa2 mission will return samples in 2020 (Kitazato et al., 2019; Sugita et al., 2019).

2. Experimental

2.1. PSD-XRD

Position sensitive detector X-ray diffraction (PSD-XRD) has previously been successfully used to investigate the mineralogy of a range of different meteorites including Y-82162 ($C1/2_{ung}$) and Y-980115 (CI1) (King et al., 2015a). Here, we have extended this work by using PSD-XRD to determine bulk mineral abundances in Y-86029 (CI1), Y-86720 ($C2_{ung}$), Y-86789 ($C2_{ung}$) and B-7904 ($C2_{ung}$).

Using the same procedure as outlined by King et al. (2015a), a ~50 mg chip (free of fusion crust) of each sample was powdered using an agate mortar and pestle to a grain size of < 35 μm, and then immediately packed into an aluminium sample holder and analysed using an INEL X-ray diffractometer equipped with a curved 120° PSD at the Natural History Museum, London (NHM). Copper $K\alpha_1$ radiation was selected with a Ge 111 monochromator, and the size of the beam was restricted using post-monochromator slits to 0.24 × 2.00 mm at the flat top of the rotating sample. XRD patterns were collected from the meteorite samples for 16 h to achieve good signal-to-noise ratios. Mineral standards for all phases identified in the meteorite XRD patterns were analysed for 30 min. Differences in the incident beam flux were monitored by measuring a polished Fe-metal block throughout the experimental run and varied by < 1% during this study.

A profile-stripping method was used to determine the abundance of each mineral phase present in the samples at typically > 1 vol% (Cressey and Schofield, 1996; Bland et al., 2004; Howard et al., 2009). For this the XRD pattern of a mineral standard was scaled to the same measurement time as the meteorite (e.g. × 32 for 16 h). The standard pattern was then reduced in intensity until it matched the intensity in the sample diffraction pattern, at which point it was subtracted to leave a residual pattern. This process was repeated for each mineral standard until zero counts remained in the residual pattern and the sum of the fit factors was one. The fit factors for the mineral standards were then corrected for relative differences in X-ray absorption to give their final volume fractions in the samples, with uncertainties < 5 vol% (e.g. King et al., 2015a).

2.2. SEM/EMPA

Secondary electron (SE) and backscattered electron (BSE) images, and energy-dispersive X-ray (EDS) element maps, were acquired from polished thin sections of Y-82162 (sample no. 45-1) and Y-980115 (sample no. 123-1) using an FEI Quanta 650 field emission gun (FEG) scanning electron microscope (SEM) equipped with a high sensitivity Bruker Flat Quad 5060 F EDS detector at the NHM. The images and maps were collected using acceleration voltages of 9 kV and 15 kV.

The composition of the matrix in Y-980115 was measured using a Cameca SX100 electron microprobe (EMPA) and wavelength-dispersive X-ray spectroscopy (WDS) at the NHM. For comparison we also analysed the matrix in the CI1 chondrite Ivuna and the CM1 chondrite LAP 02277. Spot analyses were made at random points in the matrix of each meteorite using a 1 μm beam at an acceleration voltage of 15 kV and a beam current of 20 nA. Standards included Na (jadeite), Mg (forsterite – synthetic), Al (corundum – synthetic), Si (wollastonite), P (scandium phosphate), S (barite and ZnS), K (potassium bromide), Ca (wollastonite), Ti (rutile – synthetic), Cr (chromium oxide, Cr_2O_3), Mn (manganese titanate, $MnTiO_3$), Fe (fayalite) and Ni (nickel (II) oxide). The detection limits for all elements were typically < 500 ppm and the analytical errors were ~0.1 wt%.

2.3. Noble gas analysis

Aliquots (~20 mg) of Y-82162 (×2), Y-980115 and Y-86720, and the CI chondrites Ivuna and Orgueil, were analysed for their noble gas compositions at ETH Zürich. The isotopes of He, Ne, Ar, Kr and Xe were measured in a single temperature step at ~1700 °C (for further details see Riebe et al., 2017a). Typical blanks are (in 10^{-11} cm^3 STP): 0.02, 70, 2, 6, 1500, 0.13 and 0.03 for ^{3}He, ^{4}He (increased due to a short exposure of the gas to a pressure gauge mounted in glass), ^{20}Ne, ^{36}Ar, ^{40}Ar, ^{84}Kr and ^{132}Xe, respectively. Blank contributions to the totally released gas are < 3% for He and Ne, < 1.2% for ^{36,38}Ar, ~30% for ^{40}Ar, < 1.9% for Kr and < 0.19% for Xe, respectively. The samples were fully degassed in the main temperature steps, as shown with re-extraction steps at slightly elevated temperature.

3. Results

3.1. XRD patterns and bulk mineralogy

Fig. 1 shows the PSD-XRD patterns for Y-86029, Y-86720, Y-86789 and B-7904. PSD-XRD patterns for Y-82162 and Y-980115 were reported by King et al. (2015a), and Table 1 summarises the bulk

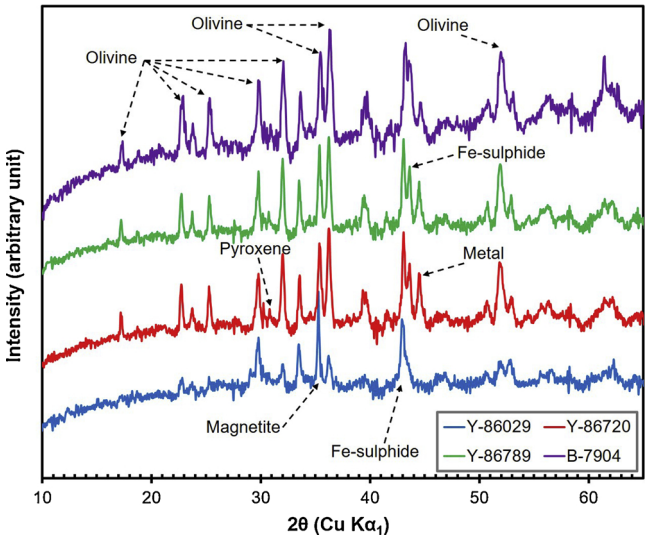

Fig. 1. PSD-XRD patterns for Y-86029, Y-86720, Y-86789, and B-7904. The main phases identified include olivine, pyroxene, magnetite, Fe-sulphide (troilite and pyrrhotite), and metal. Thermal metamorphism causes dehydration and dehydroxylation of phyllosilicates, resulting in the collapse of the phyllosilicate structure and a subsequent lack of coherent diffraction. The diffraction peaks from serpentines and smectites (e.g. at ~12°, ~19°, ~25°, and ~61°) detected for CI and CM chondrites are therefore absent.

Table 1
Bulk mineralogy of Y-82162, Y-980115, Y-86029, Y-86720, Y-86789, and B-7904 (CY chondrites) measured using PSD-XRD. Phyllosilicates are dehydrated and lack coherent diffraction in Y-82162, Y-980115, and Y-86029 (see text for details), and are absent from Y-86720, Y-86789, and B-7904. All of the meteorites contain secondary olivine that recrystallized during thermal metamorphism at temperatures > 500 °C, while B-7904 also contains primary olivine that escaped aqueous alteration.

Sample (sample no.)	Hydrated Phyllosilicates (vol %)	Dehydrated Phyllosilicates (vol %)	Primary Olivine (vol %)	Secondary Olivine (vol%)	Pyroxene (vol%)	Fe-sulphides (vol%)	Magnetite (vol%)	Metal (vol%)	Carbonates (vol%)	Other (vol%)
Y-82162* (50)		68		11		19	2			
Y-980115* (93)		71		8		19	2			
Y-86,029 (52)		67		9		19	5			
Y-86720† (61)				58	11	29		2		
Y-86789† (60)				63	7	28		2		
B-7904 (63)			20	61	6	12		1		
CY average		***34.3***	***3.3***	***35.0***	***4.0***	***21.0***	***1.0***	***0.8***		
*CI average**	*82.6*		*0.3*			*5.4*	*7.8*		*1.7*	*2.2*
CM average‡	*77.9*		*10.7*		*5.0*	*2.0*	*2.2*		*1.6*	*0.8*

* Data from King et al. (2015a); †These meteorites are described as paired by Matsuoka et al. (1996); ‡Data are from Howard et al. (2015) and King et al. (2017a).

mineralogy for all six meteorites. We also note that for Y-86029, Y-86789 and B-7904 our bulk PSD-XRD patterns (described below) are consistent with those collected from matrix samples using synchrotron XRD by Nakamura (2005) and Tonui et al. (2003; 2014).

The main phases identified in Y-86029 include olivine, Fe-sulphide (troilite), and magnetite, but the diffraction peaks associated with phyllosilicates in CI and CM chondrites (e.g. Howard et al., 2009, 2011; 2015; King et al., 2015a, 2017a) are not observed. The loss of interlayer H_2O and structural −OH transforms phyllosilicates into a highly disordered and/or very fine-grained phase that lacks coherent diffraction. This disordered phase is an indicative characteristic of aqueously altered and thermally metamorphosed carbonaceous chondrites (Nakamura, 2005; Tonui et al., 2014; King et al. 2015a).

Subtraction of olivine, Fe-sulphide and magnetite from the Y-86029 XRD pattern left a residual greater than zero, while the sum of the fit factors was less than one, indicating the presence of a highly disordered and/or very fine-grained component. We cannot fully exclude the occurrence of poorly crystalline Fe-(oxy)hydroxides and rust, however we found that the residual pattern was an excellent match to the shape and intensity (when scaled) of the diffraction pattern of our serpentine/saponite standard (excluding the diffraction peaks). We therefore attribute the remaining counts in the residual pattern to phyllosilicates that were dehydrated and dehydroxylated during thermal metamorphism. In addition, the broad reflections from olivine and Fe-sulphide suggest that these are fine-grained and/or poorly crystalline, and possibly chemically zoned secondary phases that formed through partial melting and recrystallization processes (Nakamura, 2005; Tonui et al., 2014; King et al., 2015a). The bulk mineralogy of Y-86029 is 67 vol% “dehydrated phyllosilicates”, 19 vol% Fe-sulphide, 9 vol% olivine, and 5 vol% magnetite (Table 1). The XRD pattern and bulk mineralogy of Y-86029 is very similar to the previous analyses of Y-82162 and Y-980115 published by King et al. (2015a), and agree with estimated peak metamorphic temperatures of 500–750 °C (heating stage III in the Nakamura (2005) scheme based on XRD; Tonui et al., 2003).

Phases identified in the XRD patterns of Y-86720, Y-86789 and B-7904 include olivine, pyroxene, Fe-sulphide (pyrrhotite and troilite), and metal. Olivine and Fe-sulphide reflections are still broad but more developed than in Y-86029, suggesting recrystallization at higher peak metamorphic temperatures or heating for a longer period of time (Nakamura, 2005). B-7904 also has sharp olivine reflections indicating the additional presence of crystalline primary olivine that escaped aqueous alteration (Fig. 1 and Fig. A1). Magnetite is not seen in the XRD patterns of Y-86720, Y-86789 and B-7904; this could indicate a low abundance due to less aqueous alteration (for example these meteorites all contain metal) or peak metamorphism > 570 °C, the temperature at which magnetite breaks down, in a reducing environment (Nozaki et al., 2006; Harries and Langenhorst, 2013). However, detecting low proportions of magnetite is hampered by the overlap between its main diffraction peak and the intense olivine peak at ~35° (2θ Cu $K\alpha_1$) in these meteorites (Fig. 1).

No diffraction peaks from phyllosilicates are detected for Y-86720, Y-86789 and B-7904. However, unlike for Y-86029, following subtraction of olivine, pyroxene, Fe-sulphide, and metal from the XRD patterns of Y-86720, Y-86789, and B-7904, the residuals were approximately zero counts and the sum of the fit factors was one, indicating that there was no significant contribution from a highly disordered and/or very fine-grained “dehydrated phyllosilicate” phase. The bulk mineralogy of Y-86720 and Y-86789 is ~60 vol% olivine, ~10 vol% pyroxene, ~30 vol% Fe-sulphide, plus a small amount of metal, and B-7904 is 81 vol% olivine (of which 20 vol% is primary), 6 vol% pyroxene, 12 vol% Fe-sulphide, and 1 vol% metal. Based on their XRD patterns and bulk mineralogy, we agree with previous estimates that Y-86720, Y-86789, and B-7904 are heating stage IV meteorites that experienced peak metamorphic temperatures > 750 °C (Ikeda, 1992; Matsuoka et al., 1996; Tonui et al., 2014).

3.2. Petrography and matrix compositions of Y-82162 and Y-980115

Y-82162 and Y-980115 are breccias containing mm-sized clasts, aggregates, isolated fragments and minerals, and abundant matrix. The matrix is comprised of fine-grained (< 1 μm) phyllosilicates in which grains of magnetite, Fe-sulphides, phosphates, and rare anhydrous silicate fragments are embedded. Analytical totals of the matrix are high, likely reflecting the dehydration of the phyllosilicates and recrystallization of olivine during thermal metamorphism (Table 2). Fig. 2 shows that the composition of the matrix in Y-980115 falls into two components, a mixed serpentine/smectite and a more serpentine-rich phase, and overall is intermediate to our analyses of the matrix in the highly altered CI and CM chondrites.

Coarse-grained phyllosilicate clasts are present in the matrix of Y-82162 and Y-980115, ranging from ~30 – 200 μm in size, and are angular to round in shape (Fig. 3). In most clasts the coarse-grained phyllosilicates have a fibrous appearance but in some the phyllosilicates are “tufty” in nature (Fig. 3b). The clasts contain grains of Fe-sulphide and magnetite and have a composition that is typically more Na- and Al-rich than the surrounding matrix (Fig. 3d). Large clasts of periclase up to ~700 μm in length are also found in the matrix. The periclase clasts are very fine-grained and porous, and EDS maps show that the distribution of Mg and Fe within them is highly variable (Fig. 4). Several of the periclase clasts are surrounded by a Mn-rich silicate, while others have Ca-rich rims (Fig. 4). In addition, some periclase clasts contain fine-grained Fe-sulphides, and one is cut by a vein of phyllosilicates

Table 2
Elemental composition (wt%) of the matrix in Y-82162, Y-980115, Y-86029, Y-86720, Y-86789 and B-7904 (CY chondrites), Ivuna (CI1) and LAP 02277 (CM1).

	Y-82162[†]	Y-980115[*]	Y-86029[‡]	Y-86720[†]	Y-86789[#]	B-7904[†]	Ivuna[*] (CI1)	LAP02277[*] (CM1)
SiO_2	36.2	35.0 (4.6)	37.6	39.3	45.9	33.5	33.6 (3.7)	31.5 (4.0)
TiO_2	0.1	0.1 (0.3)	0.1	0.1	0.1	0.1	0.04 (0.04)	0.1 (0.1)
Al_2O_3	2.7	2.2 (0.4)	2.4	3.0	2.2	2.9	2.9 (2.0)	2.2 (0.4)
FeO	24.3	22.7 (7.7)	25.1	19.9	18.1	26.9	18.9 (4.3)	27.8 (6.9)
NiO	2.2	1.8 (0.9)	1.9	2.1		2.6	1.5 (0.3)	1.4 (1.6)
Cr_2O_3	0.6	0.5 (0.4)	0.5	0.5	0.5	0.4	0.5 (0.2)	0.4 (0.4)
MnO	0.3	0.2 (0.2)	0.2	0.2	0.3	0.2	0.1 (0.1)	0.2 (0.04)
MgO	24.0	20.5 (2.2)	24.9	26.4	27.2	19.9	19.5 (2.3)	21.3 (4.9)
CaO	0.4	1.1 (0.7)	0.5	0.7	0.9	2.8	0.2 (0.4)	0.9 (1.8)
Na_2O	0.6	0.7 (0.2)	0.4	0.6	0.4	0.5	0.4 (0.1)	0.2 (0.1)
K_2O	0.2	0.1 (0.04)	0.1	0.1	n.d.	0.2	0.1 (0.1)	0.02 (0.02)
P_2O_5	0.04	0.1 (0.4)	0.1	0.2		0.2	0.1 (0.1)	0.1 (0.4)
Total	91.5	85.0 (3.4)	93.7	93.0	95.6	90.2	78.0 (3.1)	86.3 (3.1)
n	50	109		58		30	155	187

* Data from this study; [†]Zolensky et al. (1993); [‡]Tonui et al. (2003); [#]Matsuoka et al. (1996). *n* is the number of spot analyses and values in parentheses are 1 standard deviation. n.d. denotes not detected, and a blank space denotes not reported.

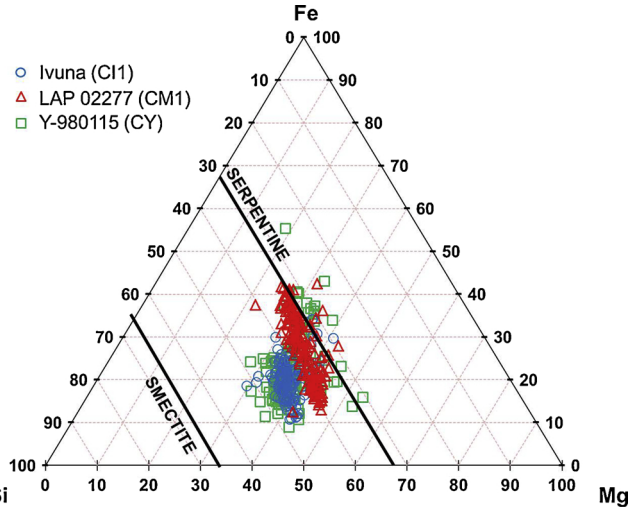

Fig. 2. Ternary diagram (element wt%) showing the composition of the matrix in Y-82162, Y-980115, the CI1 chondrites Ivuna and Alais, and the CM1 chondrite LAP 02277. The composition of the matrix in Y-82162 and Y-980115 is a mixed serpentine/smectite with average Fe/(Fe + Mg) ratios of 0.45 and 0.37, respectively.

(Fig. 5).

Magnetite is common in Y-82162 and Y-980115 either as individual grains in the matrix or aggregates ranging in size from ~20 – 60 μm. Magnetite occurs with a range of textures including euhedral crystals, framboids, spherulites, and plaquettes, sometimes with multiple morphologies found together within the same aggregate (Fig. 6), and is often associated with Fe-sulphides and phyllosilicates. Iron sulphides (pyrrhotite and troilite) are widely distributed in Y-82162 and Y-980115, present as euhedral (Fig. 7), anhedral and lath-shaped grains ranging in size from < 1 μm to > 200 μm. All of the large Fe-sulphide grains that we characterised contain Ni-rich blebs, which we interpret to be pentlandite. This pyrrhotite-pentlandite exsolution texture is common in aqueously altered and thermally metamorphosed meteorites, and our grains are very similar to the "Category B" grains described by Kimura et al. (2011), who suggested that they formed during cooling after heating to > 200 °C. At least one of the Fe-sulphide grains that we studied appears corroded, while another is rimmed by a Ca-S-rich phase that is most likely a sulphate.

Phosphates, ~10 – 30 μm in size, occur as individual grains in the matrix, within aggregates, or associated with coarse-grained phyllosilicates in Y-82162 and Y-980115 (Fig. 8). Based on the EDS maps the phosphates appear to be apatite, with several of them hosting a heterogeneous distribution of Cl (Fig. 8c). We only found two carbonate grains (~20 μm) in Y-82162 and Y-980115, in contrast to the CI and CM chondrites where carbonates, usually calcite and dolomite, are common (Endress and Bischoff, 1996; Lee et al., 2014). In both cases Mg is present and the carbonate grains are probably dolomite. They occur at the cores of larger aggregates containing Fe-sulphides, magnetite, phosphates and unidentified Mg-Si-Fe-S-bearing phases.

In addition, Y-82162 and Y-980115 contain numerous large (10's to 100's μm) unusual objects consisting of phyllosilicates, Fe-sulphides, periclase and phosphates all enclosed by thin rims of dolomite (Fig. 9). Often the whole object is mantled by what looks like an accretionary fine-grained rim (FGRs) similar to those found surrounding partially altered refractory components in CM chondrites (e.g. Trigo-Rodriguez et al., 2006). These objects could be fragments altered in, and then transported from, different regions of the parent body; however due to their shape, size and the presence of FGRs we interpret them as relict pseudomorphs formed *in-situ* from chondrules and CAIs that following accretion were fully altered on the asteroid parent body.

Numerous researchers have described Y-82162 as containing abundant matrix, large coarse-grained Na-rich phyllosilicate and periclase clasts, and widespread magnetite, Fe-sulphides, and phosphates (Tomeoka et al., 1989a; Akai, 1990; Bischoff and Metzler, 1991; Ikeda, 1991, 1992; Tonui et al., 2003, 2014). Our observations of Y-82162 are in agreement with those studies, and comparable to descriptions of Y-86029 (Tonui et al., 2003). The mineralogy and textures of Y-980115, reported here for the first time, are also very similar suggesting that there is a genetic relationship between these meteorites.

3.3. Noble gas compositions

The noble gases in all measured samples (Tables 3–6) show the expected mixture of presolar components (dominating He and Ne, Fig. 10), primordially trapped phase Q gases (dominating Ar, Kr and Xe), some terrestrial contamination best visible in the Xe isotopes (Fig. 11), and cosmogenic contributions, detectable exclusively in Ne (Fig. 10). The $^3He/^4He$ ratios, even for Y-86720 which shows the highest ratio of all the samples, are $\leq 25 \times 10^{-4}$ and thus too low to allow us to use ^3He to determine cosmic-ray exposure (CRE) ages ($(^3He/^4He)_{cos}$ ~0.2; Wieler, 2002). Most of the trapped He is of either Q/HL ($^3He/^4He$ ~1.2 – 1.7×10^{-4}, Huss and Lewis, 1994; Busemann et al., 2000) or SW-He ($^3He/^4He = (4.64 \pm 0.02) \times 10^{-4}$, Heber et al., 2009) composition. Radiogenic ^4He in unknown concentrations

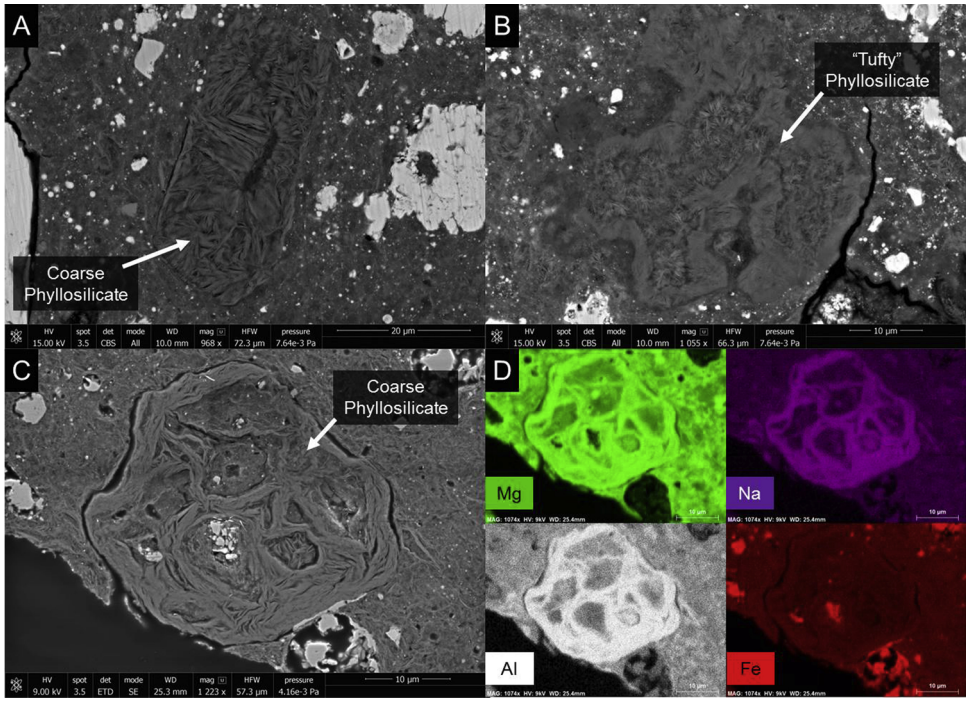

Fig. 3. (a) BSE images of a coarse-grained phyllosilicate clast in Y-980115, and (b) a coarse-grained "tufty" phyllosilicate clast in Y-980115; (c) SE image of a coarse-grained phyllosilicate clast in Y-82162, and (d) EDS maps showing the distribution of Mg, Na, Al and Fe in the phyllosilicate clast in (c).

are an additional He component, which prevents us from the decomposition of the measured He in trapped and cosmogenic He. Similarly, the measured $^{36}Ar/^{38}Ar$ ratios (Table 4) are close to 5.3 suggesting abundant Ar-Q (with $^{36}Ar/^{38}Ar = 5.34 \pm 0.02$, Busemann et al., 2000) and the additional likely present Ar-HL in presolar diamonds ($^{36}Ar/^{38}Ar = 4.41 \pm 0.06$, Huss and Lewis, 1994) prevents us from determining $^{38}Ar_{cos}$.

However, the Ne isotopes plot on mixing lines between cosmogenic and trapped Ne. Neon is a mixture of dominantly Ne-HL from diamonds, some Ne-E from presolar graphite and SiC (Lewis et al., 1994; Amari et al., 1995), potentially SW-Ne (Riebe et al., 2017b) and perhaps other trapped components (e.g. Krietsch et al., 2019). For the calculation of the cosmogenic endmember, we combined the chemistry for each chondrite (see appendix Table A1) with shielding- and chemistry-dependent model predictions for carbonaceous chondrites by Leya and Masarik (2009). The commonly used shielding indicator $(^{22}Ne/^{21}Ne)_{cos}$ cannot reliably be determined due to the overwhelming presence of trapped Ne (Fig. 10). Hence, we assumed pre-atmospheric meteoroid radii of 10 to 30 cm (and any shielding depth). The recovered mass of the largest meteorite measured here, Orgueil, would resemble a meteoroid of 11 cm radius. All production rates, $^{20}Ne/^{22}Ne$ and $^{21}Ne/^{22}Ne$ ratios resulting for these conditions from the chosen

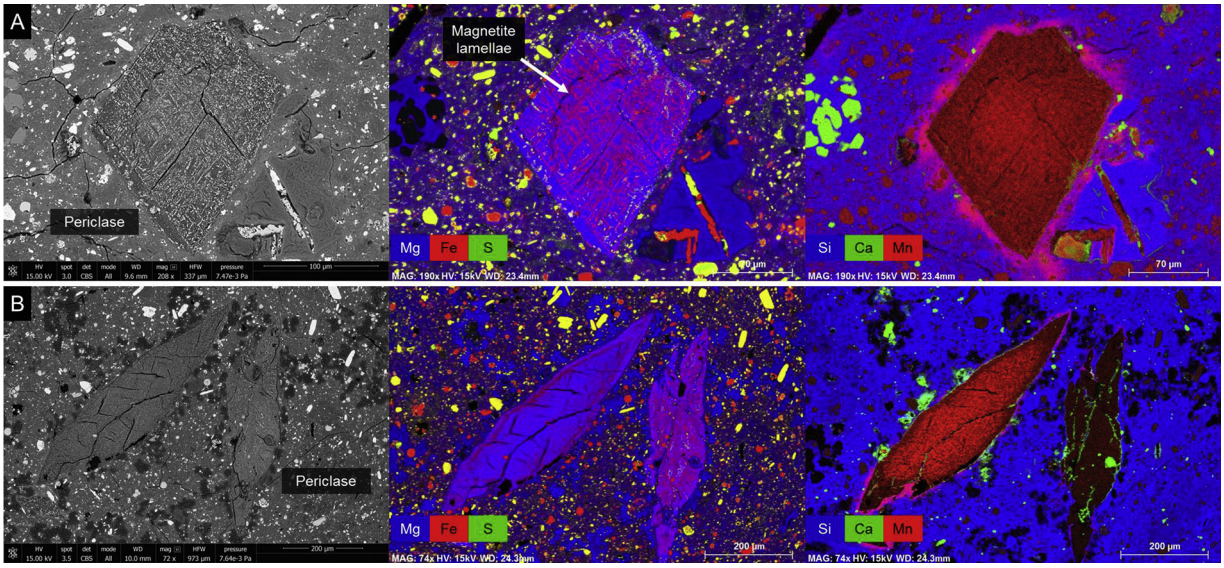

Fig. 4. BSE images (left) and corresponding EDS maps showing the distribution of Mg (B), Fe (R), and S (G) (middle), and Si (B), Ca (G), and Mn (R) (right) in periclase clasts within (a) Y-980115 and (b) Y-82162.

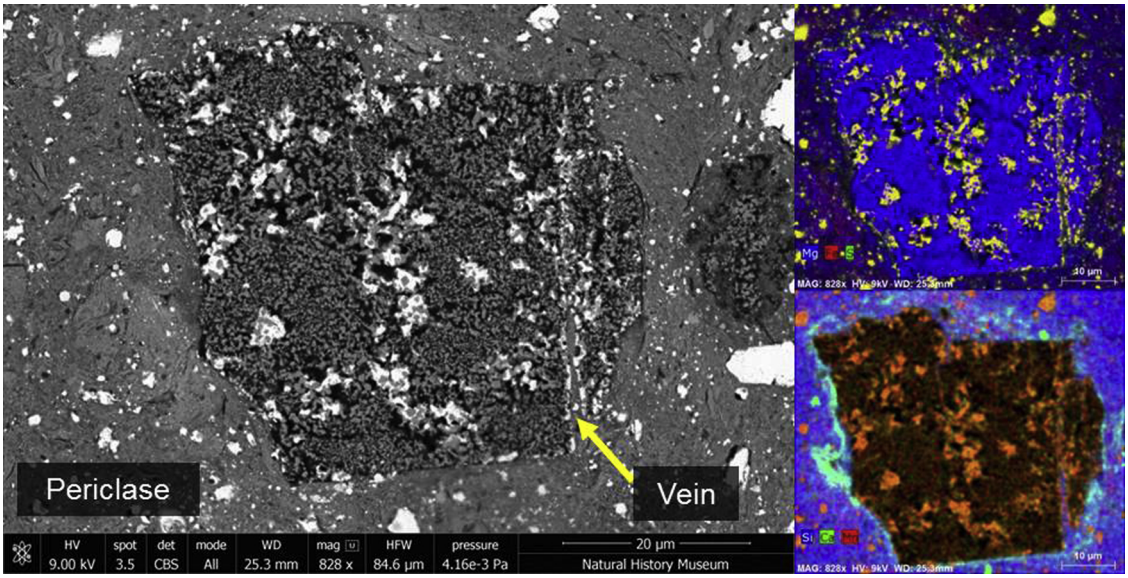

Fig. 5. BSE image and corresponding EDS maps showing the distribution of Mg (B), Fe (R) and S (G) (top right), and Si (B), Ca (G) and Mn (R) (bottom right) in a periclase clast within Y-82162. The clast is dotted with Fe-sulphides and cut by a vein of phyllosilicates with the same composition as the surrounding matrix.

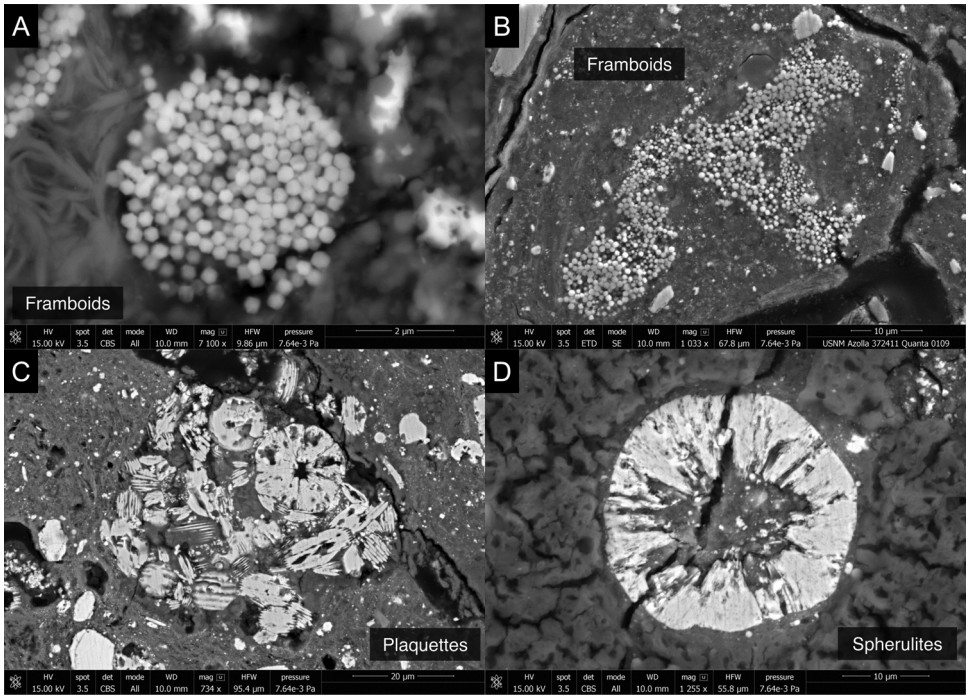

Fig. 6. BSE images showing examples of magnetite (a, b) framboids, (c) plaquettes, and (d) spherulites in Y-980115 and Y-82162.

chemistry (see Table A1) were used.

Both our and a literature data point (Weber and Schultz (1991)) of Y-82162 plot on a mixing line between cosmogenic Ne and Ne-HL, and we thus used HL (Huss and Lewis, 1994) as the trapped endmember to determine the cosmogenic ^{21}Ne concentration in this meteorite. For the other chondrites (including literature data from Nagao et al., 1984 and Weber and Schultz (1991)) we extrapolated linear fits through the measured Ne ratios and the cosmogenic endmember to a $(^{21}Ne/^{22}Ne)_{tr}$ ratio = 0.0327 (average of Q and HL composition, the choice of which is not critical) to receive the corresponding $(^{20}Ne/^{22}Ne)_{tr}$ for each meteorite (Table 3). Using these endmembers, we calculated the cosmogenic and trapped Ne concentrations given in Table 3. CRE ages (Table 7) are calculated based on these $^{21}Ne_{cos}$ concentrations and corresponding production rates obtained with the model by Leya and Masarik (2009) and the bulk chemical composition listed in Table A1.

4. Discussion

The carbonaceous chondrites Y-82162, Y-980115, Y-86029, Y-86720, Y-86789 and B-7904 have similar mineralogical, textural, and chemical characteristics. All of these meteorites record a period of intense aqueous alteration that was followed by at least one thermal metamorphic event at temperatures > 500 °C. In the following sections we combine our new mineralogical, petrographic, and noble gas

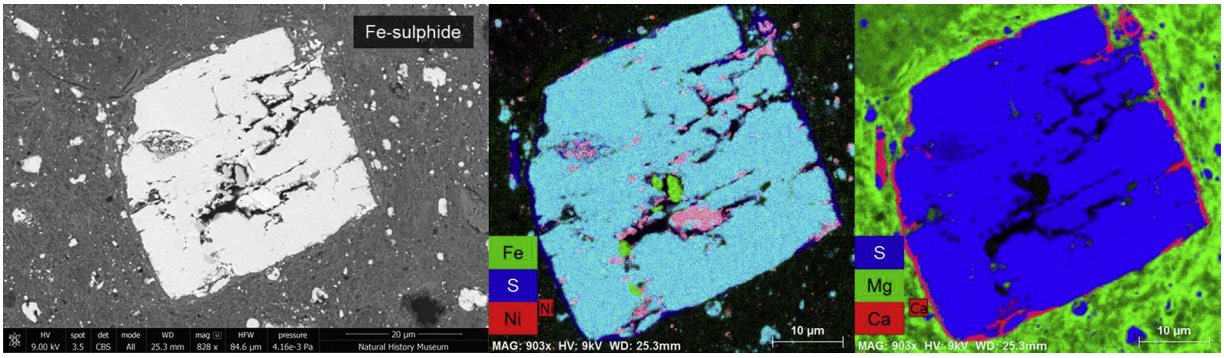

Fig. 7. BSE image (left) and corresponding EDS maps showing the distribution of Fe (G), S (B), and Ni (R) (middle), and S (B), Mg (G), Ca (R) (right), in an Fe-sulphide grain in Y-82162. The grain contains pentlandite blebs and is rimmed by a Ca-S-rich phase that it likely a sulphate.

analyses with literature data and describe the evidence that justifies these meteorites forming a group – the CYs – that is unique from other carbonaceous chondrites.

4.1. Oxygen isotopic compositions

The bulk oxygen isotopic composition of meteorites is controlled by the composition of the starting materials and chemical processing, either in the protoplanetary disk or on the parent body. Bulk oxygen isotopic composition is one of the main criteria used for classifying carbonaceous chondrites into different groups, although some overlap between the groups does exist. The bulk oxygen isotopic compositions of Y-82162, Y-86029, Y-86720, Y-86789, and B-7904 (to our knowledge there are no oxygen data for Y-980115) are very similar to one another, with values of $\delta^{17}O$ ~12‰ and $\delta^{18}O$ ~22‰ (Clayton and Mayeda, 1999; Tonui et al., 2014). Plotting above the CI chondrite field and close to the intersection of the terrestrial fractionation and CM mixing lines (Fig. 12), the oxygen isotopic compositions of these meteorites are the heaviest measured in any meteorite group.

Y-82162, Y-86029, Y-86720, Y-86789 and B-7904 all experienced aqueous alteration and thermal metamorphism, processes that would strongly influence their bulk oxygen isotopic compositions. The effects of low temperature (< 200 °C) aqueous alteration on the oxygen isotopic composition of carbonaceous chondrites are generally well constrained, with reactions between isotopically "light" anhydrous silicates and "heavy" fluids resulting in progressively heavier bulk compositions with increasing hydration (Clayton and Mayeda, 1999). In contrast, the effects of thermal metamorphism and subsequent dehydration of phyllosilicates remain poorly understood, in part complicated by kinetics, potential isotopic partitioning between vapour and residual solids, and the role of organic matter (Clayton et al., 1997; Clayton and Mayeda, 2009; Tonui et al., 2014). Nevertheless, it has been shown that thermal metamorphism causes preferential loss of isotopically light water and associated heavy isotope enrichment in the solids (Valley et al., 1986; Clayton and Mayeda, 1999, 2009). Thus, both hydration and dehydration of carbonaceous chondrites should cause bulk oxygen

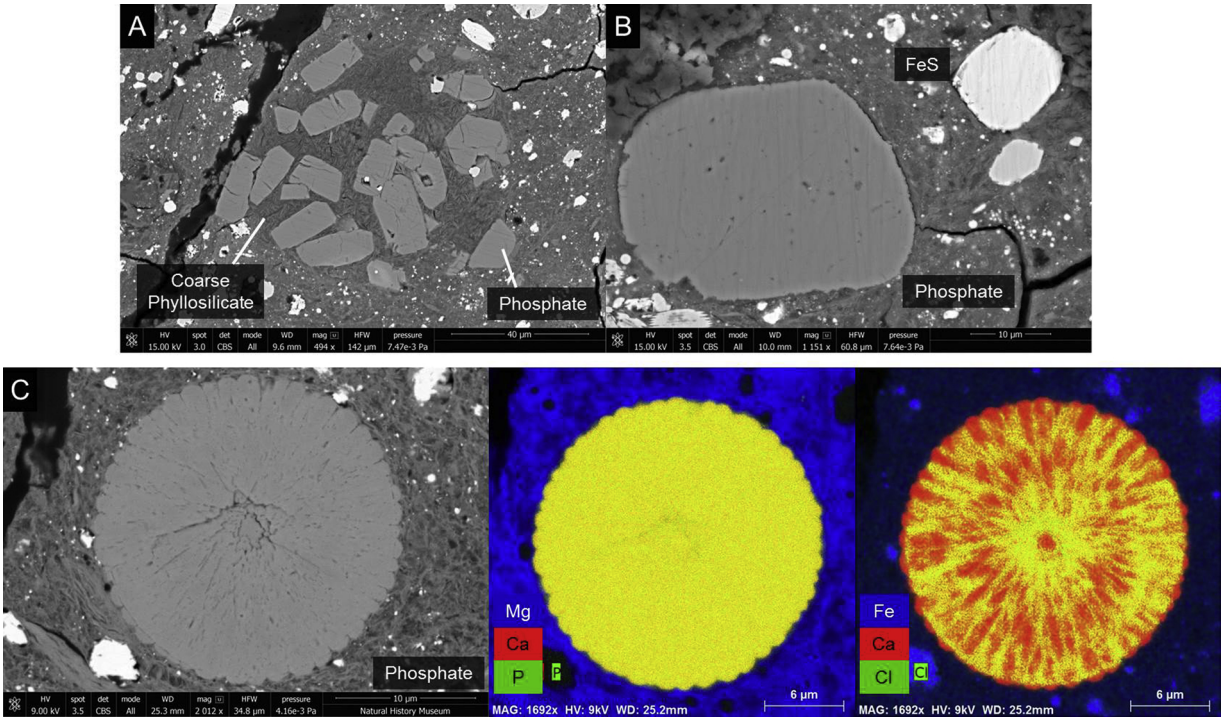

Fig. 8. BSE images of phosphate grains (a) associated with a coarse-grained phyllosilicate clast, and (b) in the matrix of Y-980115; (c) BSE image (left) and corresponding EDS maps showing the distribution of Mg (B), Ca (R), and P (G) (middle), and Fe (B) and Cl (R) (right) in a phosphate grain within Y-82162.

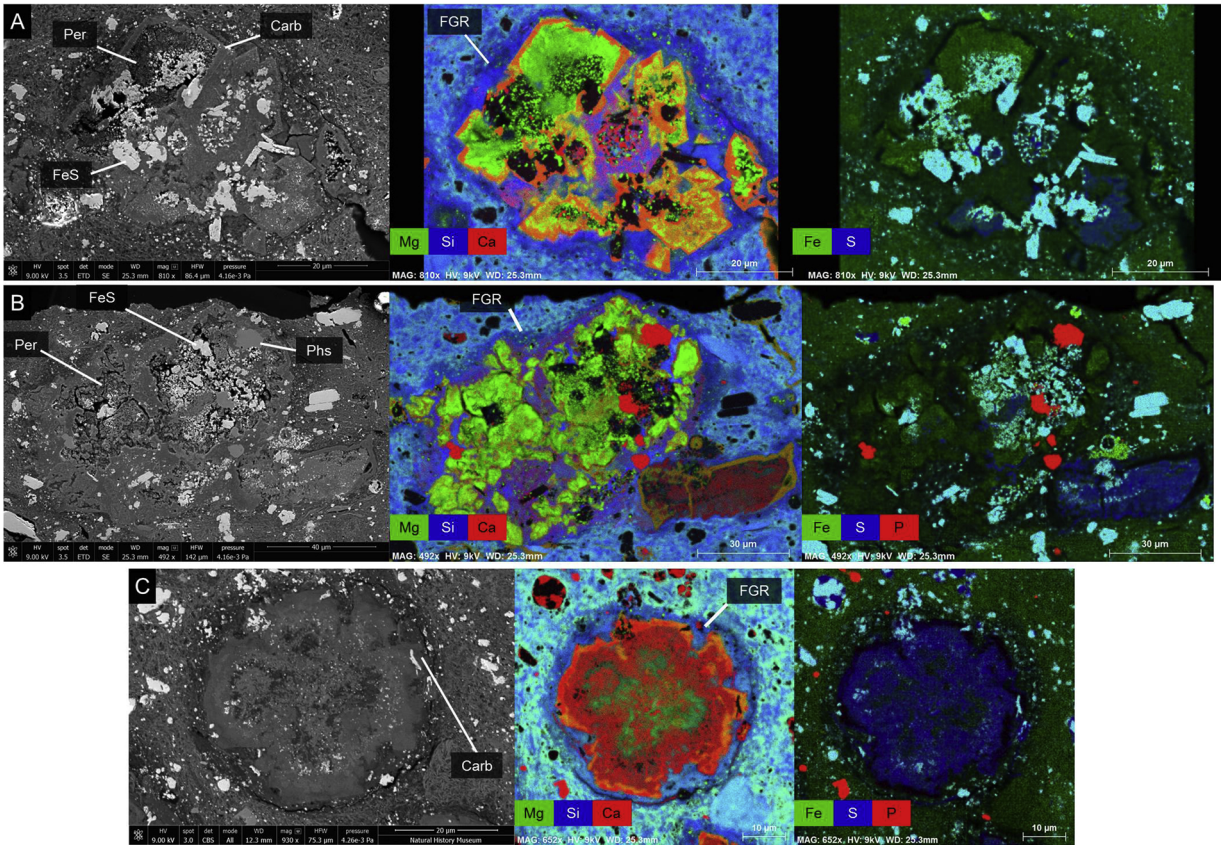

Fig. 9. (a) and (b) are SE images (left) and corresponding EDS maps showing the distribution of Mg (G), Si (B) and Ca (R) (middle), and Mg (G), S (G) and P (R) (right) in objects consisting of phyllosilicates, Fe-sulphides (FeS), periclase (Per) and phosphates (Phs) enclosed by carbonates (Carb) within Y-82162; (c) BSE image (left) and corresponding EDS maps showing the distribution of Mg (G), Si (B) and Ca (R) (middle), and Mg (G), S (G) and P (R) (right) in an object consisting of phyllosilicates, Fe-sulphides, periclase and phosphates enclosed by carbonates in Y-82162. The objects appear to be relict chondrules and/or CAIs and are surrounded by fine-grained rims (FGR) of materials with compositions distinct from the matrix.

isotopic compositions to become enriched in the heavy isotopes.

The heavy oxygen isotopic composition of Y-82162, Y-86029, Y-86720, Y-86789 and B-7904 supports the conclusion that they experienced intense periods of parent body aqueous alteration and thermal metamorphism. Analyses of artificially heated samples (under vacuum in a sealed glass tube and heated with a furnace to 400 °C, 500 °C, 600 °C, 700 °C, 800 °C and 1000 °C) of the CM chondrite Murchison and terrestrial analogues showed an initial increase in $\delta^{18}O$ of ~2 – 4‰, with little further change in the composition of samples heated to > 500 °C (Clayton et al., 1997; Clayton and Mayeda, 2009). The artificial heating experiments may not have perfectly replicated asteroid conditions, but the $\delta^{18}O$ values of Y-82162, Y-86029, Y-86720, Y-86789, and B-7904 are ~6‰ higher than the CIs, leading to suggestions that at least some of

Table 4
Argon concentrations (in 10^{-8} cm^3 STP/g) and isotopic ratios in Y-82162 (two aliquots), Y-980115, Y-86720, and the CI chondrites Ivuna and Orgueil.

	^{36}Ar	$^{36}Ar/^{38}Ar$	$^{40}Ar/^{36}Ar$
Y-82162-a	72.90 ± 1.89	5.238 ± 0.027	3.33 ± 1.09
Y-82162-b	80.65 ± 4.20	5.328 ± 0.026	6.91 ± 0.37
Y-980115	89.37 ± 2.30	5.257 ± 0.028	5.71 ± 0.99
Y-86720	41.76 ± 2.67	5.331 ± 0.025	6.60 ± 0.43
Ivuna	106.99 ± 3.14	5.312 ± 0.031	2.67 ± 0.62
Orgueil	105.69 ± 3.09	5.329 ± 0.022	2.83 ± 0.66

See Table 3 for details of uncertainties.

Table 3
Helium and Ne concentrations (in 10^{-8} cm^3 STP/g) and isotopic ratios in Y-82162 (two aliquots), Y-980115, Y-86720, and the CI chondrites Ivuna and Orgueil.

	Mass	^{4}He	$^{3}He/^{4}He$	^{20}Ne	$^{20}Ne/^{22}Ne$	$^{21}Ne/^{22}Ne$	$^{20}Ne_{tr}$	$^{21}Ne_{cos}$
	mg		× 10000					
Y-82162-a	18.59 ± 0.03	4904 ± 28	1.596 ± 0.018	19.63 ± 0.28	8.441 ± 0.065	0.04979 ± 0.00045	19.525 ± 0.039	0.0240 ± 0.0082
Y-82162-b	20.91 ± 0.02	5003 ± 66	1.591 ± 0.025	19.95 ± 0.23	8.593 ± 0.047	0.04784 ± 0.00035	19.709 ± 0.040	0.0021 ± 0.0091
Y-980115	16.71 ± 0.02	4852 ± 26	1.666 ± 0.020	24.69 ± 0.29	8.890 ± 0.036	0.05195 ± 0.00072	23.77 ± 0.81	0.0555 ± 0.0049
Y-86720	21.11 ± 0.01	267.44 ± 3.61	25.09 ± 0.41	2.86 ± 0.06	5.186 ± 0.095	0.2382 ± 0.0020	3.15 ± 0.41	0.1179 ± 0.0027
Ivuna	19.84 ± 0.03	10105 ± 150	3.656 ± 0.058	28.29 ± 0.36	6.819 ± 0.039	0.1426 ± 0.0010	27.831 ± 0.077	0.4740 ± 0.0093
Orgueil	21.33 ± 0.02	22989 ± 243	3.902 ± 0.047	48.63 ± 0.69	8.171 ± 0.063	0.1803 ± 0.0011	47.79 ± 5.60	0.435 ± 0.013

Uncertainties of measured concentrations include those of counting statistics, sample masses, and blanks and detector sensitivity. Uncertainties of isotopic ratios include those of counting statistics, blank corrections, and instrumental mass discrimination. Uncertainties of cosmogenic and trapped concentrations include the uncertainties of the deconvolution, i.e., the choice of the endmember components and all experimental uncertainties.

Table 5
Krypton concentrations (in 10^{-10} cm^3 STP/g) and isotopic ratios in Y-82162 (two aliquots), Y-980115, Y-86720, and the CI chondrites Ivuna and Orgueil.

	^{84}Kr	^{78}Kr/^{84}Kr	^{80}Kr/^{84}Kr	^{82}Kr/^{84}Kr	^{83}Kr/^{84}Kr	^{86}Kr/^{84}Kr
				^{84}Kr = 100		
Y-82162-a	107.40 ± 2.63	0.5968 ± 0.0092	3.883 ± 0.043	20.26 ± 0.22	20.19 ± 0.21	30.67 ± 0.33
Y-82162-b	146.81 ± 1.23	0.5862 ± 0.0058	3.910 ± 0.030	19.92 ± 0.12	19.76 ± 0.13	30.54 ± 0.18
Y-980115	120.18 ± 2.89	0.6027 ± 0.0086	3.947 ± 0.042	19.91 ± 0.19	19.98 ± 0.16	30.47 ± 0.31
Y-86720	52.13 ± 0.42	0.5850 ± 0.0086	3.823 ± 0.043	19.97 ± 0.21	20.01 ± 0.21	30.29 ± 0.35
Ivuna	116.84 ± 2.89	0.6057 ± 0.0087	3.904 ± 0.053	19.93 ± 0.22	20.41 ± 0.29	30.73 ± 0.35
Orgueil	119.50 ± 2.83	0.5959 ± 0.0079	3.901 ± 0.044	19.74 ± 0.19	20.06 ± 0.19	30.25 ± 0.28

See Table 3 for details of uncertainties.

these meteorites could be examples of thermally metamorphosed CI chondrites (Ikeda, 1992; Clayton and Mayeda, 1999). However, while we agree that they were heavily-altered, phyllosilicate-rich rocks prior to heating our petrographic observations (see Section 4.5) are not consistent with them being CI chondrites.

4.2. Elemental compositions and H_2O contents

The major and trace element compositions of Y-82162, Y-980115 and Y-86029 are similar to the CI chondrites, whereas the composition of Y-86720, Y-86789 and B-7904 are closer to the CMs (Haramura et al., 1983; Kallemeyn, 1988; Ebihara and Shinonaga, 1989; Tomeoka et al., 1989a, 1989b; Tonui et al., 2003; Braukmüller et al., 2018). Element concentrations and the ratio of elements with different volatilities (e.g. Zn/Mn, Sc/Mn) can be taxonomically indicative (e.g. Kallemeyn and Wasson, 1981; Friedrich et al., 2018). However, elemental compositions, and in particular trace elements, are modified by aqueous alteration and, to an even greater extent, thermal metamorphism. For example, Fig. 13 shows that Y-82162, Y-980115, Y-86029, Y-86720, Y-86789 and B-7904 are all significantly depleted in the most volatile elements relative to CI concentrations, indicating loss during open system thermal metamorphism. In particular, the depletions of In, Bi, Tl and Cd in Y-82162, Y-980115 and Y-86029 are consistent with analyses of the Murchison (CM) meteorite artificially heated to temperatures of 500–700 °C (Y-86029 < Y-980115 < Y-82162 (highest peak temperature); Paul and Lipschutz, 1990; Tonui et al., 2003, 2014; Braukmüller et al., 2018). Y-86720 and Y-86789 additionally show a depletion in Zn implying thermal metamorphism at temperatures > 700 °C (Paul and Lipschutz, 1990).

Previous studies have shown that Y-82162 and Y-980115 contain ~5 – 10 wt% H_2O, while Y-86720 and B-7904 contain < 5 wt% (Haramura et al., 1983; Tomeoka et al., 1989a, 1989b; King et al., 2015b; Braukmüller et al., 2018). Even taking into account the potential terrestrial contribution to these analyses, the H_2O contents of Y-82162, Y-980115, Y-86720 and B-7904 are clearly depleted relative to the CI (which contain ~20 wt%) and CM (~15 wt%) chondrites, which again can be attributed to them having undergone thermal metamorphism at temperatures > 500 °C (Ikeda, 1992; King et al., 2015b). The lower H_2O contents of Y-86720 and B-7904 perhaps suggests that these meteorites were heated to even higher temperatures (consistent with mineralogical and petrographic characteristics), but could also reflect heating for a longer period of time, or variations in the degree of aqueous alteration, and hence H_2O abundance, prior to dehydration.

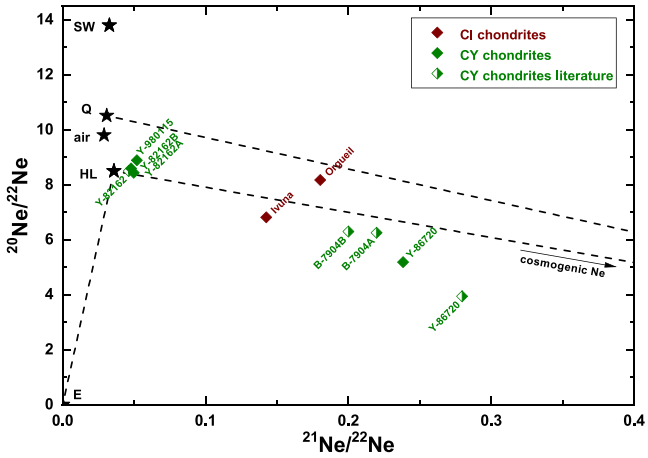

Fig. 10. Neon compositions in Y-82162 (two aliquots), Y-980115, Y-86720 (CY chondrites), and the CI chondrites Ivuna and Orgueil. Literature data are from Nagao et al. (1984) and Weber and Schultz (1991).

4.3. Noble gas abundances and compositions

Noble gas concentrations support the view that Y-82162, Y-980115 and Y-86720 underwent severe thermal metamorphism resulting in volatile loss, relative to CI compositions, and, moreover that Y-86720 (measured here) and B-7904 (measured by Nagao et al., 1984 and Weber and Schultz (1991)) experienced higher temperatures than Y-82162 and Y-980115, or the same temperatures but for a longer period of time. Trapped ^{20}Ne (in 10^{-8} cm^3/g) decreases with thermal metamorphism from the unheated CI chondrites Ivuna and Orgueil (28 and 48) to Y-980115 (24), Y-82162 (20), and finally B-7904 (9–10) and Y-86720 (3). We observe similar sequences for ^{36}Ar and ^{84}Kr concentrations (Tables 3–6), with the highest found in the CI chondrites and by

Table 6
Xenon concentrations (10^{-10} cm^3 STP/g) and isotopic ratios in Y-82162 (two aliquots), Y-980115, Y-86720, and the CI chondrites Ivuna and Orgueil.

	^{132}Xe	^{124}Xe/^{132}Xe	^{126}Xe/^{132}Xe	^{128}Xe/^{132}Xe	^{129}Xe/^{132}Xe	^{130}Xe/^{132}Xe	^{131}Xe/^{132}Xe	^{134}Xe/^{132}Xe	^{136}Xe/^{132}Xe
		^{132}Xe = 100							
Y-980115	293.15 ± 7.79	0.3949 ± 0.0029	0.3527 ± 0.0016	7.483 ± 0.044	102.24 ± 0.55	15.490 ± 0.086	80.47 ± 0.33	38.97 ± 0.16	33.06 ± 0.13
Y-82162A	240.92 ± 6.45	0.3923 ± 0.0033	0.3555 ± 0.0025	7.428 ± 0.037	100.35 ± 0.51	15.267 ± 0.070	79.37 ± 0.42	38.56 ± 0.24	32.59 ± 0.24
Y-82162B	333.56 ± 5.84	0.3867 ± 0.0040	0.3532 ± 0.0034	7.537 ± 0.057	99.92 ± 0.86	15.75 ± 0.12	80.89 ± 0.62	39.65 ± 0.32	33.88 ± 0.27
Y-86720	112.01 ± 2.03	0.3772 ± 0.0047	0.3504 ± 0.0033	7.370 ± 0.069	98.19 ± 1.00	15.23 ± 0.14	79.76 ± 0.74	38.26 ± 0.35	32.09 ± 0.30
Ivuna	137.16 ± 3.72	0.4625 ± 0.0050	0.4082 ± 0.0040	8.352 ± 0.075	107.07 ± 0.81	16.39 ± 0.14	82.34 ± 0.65	38.64 ± 0.29	32.24 ± 0.23
Orgueil	140.95 ± 3.80	0.4477 ± 0.0041	0.4024 ± 0.0039	8.188 ± 0.058	106.13 ± 0.87	16.054 ± 0.087	81.59 ± 0.47	38.32 ± 0.25	31.97 ± 0.19

See Table 3 for details of uncertainties.

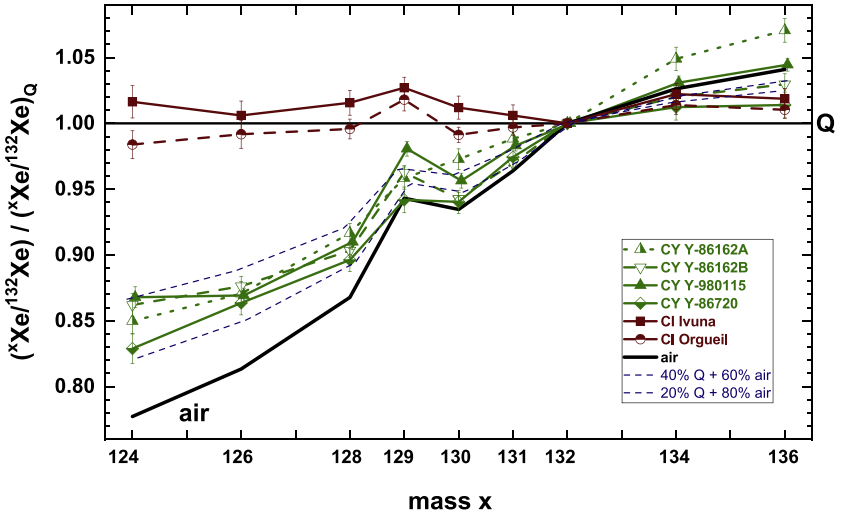

Fig. 11. Xenon isotopic compositions of Y-82162 (two aliquots), Y-980115, Y-86720 (CY chondrites), and the CI chondrites Ivuna and Orgueil. The compositions are normalised to Xe-Q from Busemann et al. (2000).

Table 7
Cosmic-ray exposure ages T_{21} determined for the CI chondrites Ivuna and Orgueil, and Y-82162, Y-980115, Y-86720, and B-7904 measured here and in the literature, and production rates P_{21} determined based on a pre-atmospheric radius of 10–30 cm, all possible shielding (see main text), and the chemistry given in the appendix Table A1 using the model of Leya and Masarik (2009). Uncertainties include those of the measurements, the component de-composition and shielding. The uncertainties of the modelling are not included and estimated to be 20%.

	reference	$P_{21}[10^{-8}$ cm^{3}STP/(g*Ma)]	T_{21} [Ma]
Y-82162-a	this work	0.192 ± 0.063	0.13 ± 0.06
Y-82162-b	this work	0.192 ± 0.063	≤0.06
Y-82162	Weber and Schultz (1991)	0.192 ± 0.063	0.06 ± 0.05
Y-980115	this work	0.188 ± 0.060	0.30 ± 0.10
Belgica 7904	Weber and Schultz (1991)	0.217 ± 0.073	1.45 ± 0.49
Belgica 7904	Nagao et al., 1984	0.217 ± 0.073	1.18 ± 0.40
Y-86720	this work	0.212 ± 0.071	0.56 ± 0.19
Y-86720	Weber and Schultz (1991)	0.212 ± 0.071	0.49 ± 0.17
Ivuna	this work	0.156 ± 0.051	3.03 ± 1.00
Orgueil	this work	0.156 ± 0.051	2.78 ± 0.92

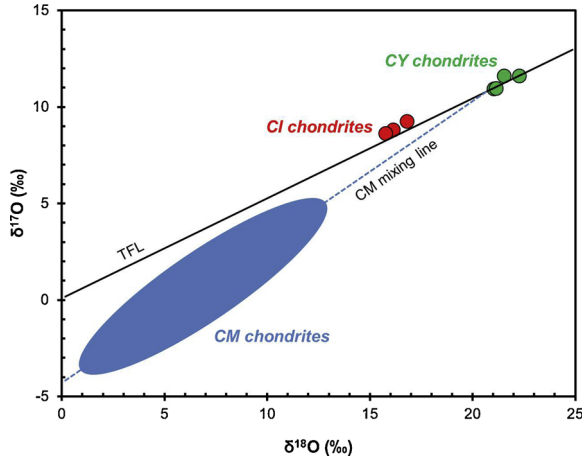

Fig. 12. Bulk oxygen isotopic compositions of Y-82162, Y-86029, Y-86720, Y-86789, and B-7904 (CY chondrites) compared to the CI and CM chondrite fields. TFL = Terrestrial Fractionation Line. Data are from Clayton and Mayeda (1999) and Tonui et al. (2014).

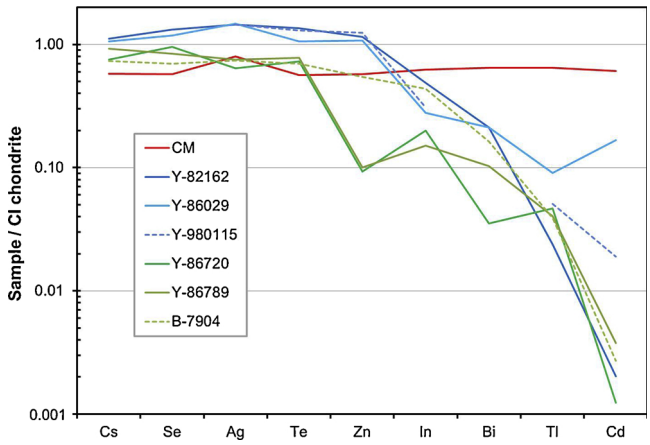

Fig. 13. Abundance of mobile trace elements in Y-82162, Y-980115, Y-86029, Y-86720, Y-86789, and B-7904. Also shown is the average abundance of the same elements for the CM chondrites. Y-82162, Y-980115, Y-86029, Y-86720, Y-86789, and B-7904 are depleted in Zn, In, Bi, Tl and Cd relative to CI (from Barrat et al., 2012), consistent with thermal metamorphism at temperatures > 500 °C. Data are from Paul and Lipschutz (1990); Tonui et al. (2003), and Braukmüller et al. (2018).

far the lowest in Y-86720. The loss in volatile elements experienced by B-7904 and Y-86720 is visible in all the noble gases.

In ^{84}Kr and ^{132}Xe another effect is discernible (Tables 5 and 6), which affected all of the Antarctic meteorite finds compared to the falls Orgueil and Ivuna, and partially overprints the above trend. This is terrestrial weathering that leads to significantly higher Kr and Xe concentrations in the Antarctic meteorites than in the falls. Fig. 11 shows the Xe isotopic compositions of all meteorites analysed here normalised to Xe-Q (Busemann et al., 2000) and clearly highlights the impact of terrestrial Xe on the Antarctic samples. The Antarctic meteorites incorporated between 60 and 80% of the released Xe from terrestrial air, whereas the CI chondrite falls show roughly Xe-Q composition. Additional Xe-HL enriched in the lightest and heaviest isotopes of Xe from presolar diamonds (Huss and Lewis, 1994) could be responsible for further variations for Q and air in particular ^{134}Xe/^{132}Xe and ^{136}Xe/^{132}Xe. The Ar in Y-82162, Y-980115 and Y-86720 is essentially unaffected by terrestrial contamination as shown by ^{40}Ar/^{36}Ar ratios between 3.3 and 6.9 (^{40}Ar/^{36}Ar in air is 296). The radiogenic ^{4}He concentration in Y-86720 is remarkably low (Table 3), which suggests

that the volatile loss due to thermal metamorphism in this meteorite occurred comparably late.

CRE ages typically represent the time the meteoroids remained in space after ejection from the parent body and before atmospheric entry. Clustering of ages could indicate that the respective samples were ejected from the parent body by the same event. The ages that could be determined only for cosmogenic ^{21}Ne (see Section 3.3), are different for Ivuna and Orgueil than they are for Y-82182, Y-980115, Y-86720 and B-7904. This possibly supports the hypothesis that these two groups of meteorites are derived from different parent bodies, although obviously the statistics are limited. Y-82162, Y-980115, Y-86720 and B-7904 could originate from three or four distinct ejection events, with Y-82162 and Y-980115 having the shortest exposure ages of < 0.2 and ~0.3 Ma, respectively. This could imply that these two meteorites are source-crater paired, and their bulk mineralogy (see Section 4.4) and petrographic characteristics (see Section 4.5) are very similar. The most heated samples Y-86720 and B-7904 (for consistency literature data were recalculated, see footnote for Table A1) have CRE ages of ~0.5 and 1.3 Ma, respectively, and, hence, most likely came from different events. The CI chondrites have longer CRE ages (≥2.8 Ma, cf. also, e.g., Herzog and Caffee, 2014). Nevertheless, all of these calculated CRE ages are still very short compared to most other meteorite classes and may imply that Y-82162, Y-980115, Y-86720, B-7904 and the CI chondrites originate from Earth-crossing asteroids rather than the main asteroid belt (Eugster, 2003).

4.4. Bulk mineralogy

King et al. (2015a) reported that Y-82162 and Y-980115 contain ~70 vol% "dehydrated phyllosilicate", ~20 vol% Fe-sulphide, ~10 vol% olivine, and ~2 vol% magnetite. The XRD pattern and bulk mineralogy of Y-86029 is very similar, and although this does not determine whether these meteorites are paired, we can infer that they reached heating stage III (500–750 °C). The lack of coherent diffraction indicates that the phyllosilicates are dehydrated and dehydroxylated, and broad olivine and Fe-sulphide reflections are consistent with recrystallization during thermal metamorphism. No crystalline, primary olivine was detected in Y-82162, Y-980115 and Y-86029 suggesting that they experienced near-complete aqueous alteration. If all the olivine is considered to be a secondary product of thermal metamorphism, then we estimate that prior to heating Y-82162, Y-980115 and Y-86029 contained ~80 vol% phyllosilicate (i.e. "dehydrated phyllosilicate plus secondary olivine, corrected for volume change; King et al., 2015a), comparable to the highly altered CI1 and CM1 chondrites (King et al., 2015a, 2017a).

It has been proposed that Y-86720 and Y-86789 are paired meteorites (Matsuoka et al., 1996), and we find that their XRD patterns and bulk mineralogy are very similar to one another. The abundance of secondary olivine (~60 vol%), Fe-sulphide (~30 vol%), and metal (~2 vol %) is consistent with classification as heating stage IV (> 750 °C). Neither meteorite contains a significant "dehydrated phyllosilicate" component, although these have been observed in transmission electron microscope (TEM) studies of the matrix (Tomeoka et al., 1989b). They contain pyroxene (~10 vol%), but in both cases the peak is relatively small and the PSD-XRD method is not optimised for high resolution analysis of peak widths, and thus it is difficult to assign it to a primary, unaltered phase or secondary from the metamorphism. However, Nakamura (2005) identified poorly crystalline pyroxene in an XRD pattern of Y-86789 suggesting that it is a secondary phase. Furthermore pyroxene, as a Mg-rich mineral, was among the last phases to be altered by fluids in the CM chondrites (Hanowski and Brearley, 2001; Velbel et al., 2012, 2015), while we find no evidence for primary olivine in Y-86720 and Y-86789. If indeed the pyroxene is secondary, this would suggest that Y-86720 and Y-86789 underwent complete hydration and had pre-metamorphism phyllosilicate abundances of ~70 vol%. This abundance is similar to the CM2 chondrites, although these are only partially altered and usually also consist of ~25 vol% primary anhydrous silicates (olivine and pyroxene) (Howard et al., 2009, 2011, 2015). B-7904 is a heating stage IV meteorite, containing 81 vol% olivine, 12 vol % Fe-sulphide, 6 vol% pyroxene, 1 vol% metal and no "dehydrated phyllosilicate". However, 20 vol% of the olivine is primary, indicating that B-7904 experienced only partial aqueous alteration and likely contained ~70 vol% phyllosilicate and at least 20 vol% olivine before heating.

We argue that the bulk mineralogy of Y-82162, Y-980115, Y-86029, Y-86720, Y-86789, and B-7904 prior to thermal metamorphism probably resembled the CI and CM chondrites. The presence of primary olivine in some members of the group but not others suggests that they cover the petrologic range from type 2 to type 1 chondrites. However, the bulk mineralogy of Y-82162, Y-980115, Y-86029, Y-86720, Y-86789, and B-7904 is distinct from the CI and CMs in several ways, some of which, such as the abundance of metal, can be attributed to severe thermal metamorphism under reducing conditions on the parent body (Nakamura 2005). The abundance of magnetite is more complex as it can form through aqueous alteration and thermal decomposition of tochilinite and Fe-rich phyllosilicates, but also breaks down at temperatures > 570 °C (Harries and Langenhorst, 2013). The main difference is the abundance of Fe-sulphide, which is considerably higher (~10 – 30 vol%) in Y-82162, Y-980115, Y-86,029, Y-86720, Y-86789, and B-7904 than the CI (~5 vol%; King et al., 2015a) or CM chondrites (< 5 vol%; Howard et al., 2009, 2011, 2015; King et al., 2017a). In the thermally metamorphosed CMs, Fe-sulphides are believed to form through the decomposition (> 120 °C) of tochilinite (Nakamura, 2005; Kimura et al., 2011), a phase that is absent from the CI chondrites. Tomeoka et al. (1989a, 1989b) and Ikeda (1992) found high Fe-sulphide abundances, comparable to those reported here, in Y-82162, Y-86720 and B-7904 and proposed that their pre-alteration mineralogy differed from the CI and CM chondrites. We agree and suggest that the bulk mineralogy of Y-82162, Y-980115, Y-86029, Y-86720, Y-86789, and B-7904 cannot be attributed to the effects of thermal metamorphism alone, and instead attests to them having a different starting mineralogy and/or alteration history.

4.5. Petrographic characteristics

Y-82162 and Y-980115 are breccias containing abundant fine-grained matrix, magnetite, Fe-sulphides, phosphates, and periclase. Our observations of Y-82162 are in agreement with previous studies (Tomeoka et al., 1989a; Akai, 1990; Bischoff and Metzler, 1991; Ikeda, 1991, 1992; Tonui et al., 2003, 2014), and suggest that these two meteorites are closely related. The detailed description provided by Tonui et al. (2003) indicates that the mineralogy and textures of Y-86029 are also very similar. The matrix in Y-82162, Y-980115 and Y-86029 largely consists of mixed serpentine/smectite (Fig. 2; Tomeoka et al., 1989a; Akai, 1990; Bischoff and Metzler, 1991; Ikeda, 1991; Tonui et al., 2003), although the phyllosilicates were dehydrated by thermal metamorphism, as evidenced by their high analytical totals (Table 2). The composition of the matrix and the abundance and morphology of magnetite suggest that Y-82162, Y-980115 and Y-86029 are highly altered meteorites that were comparable to CI1 chondrites prior to thermal metamorphism. However, we propose that several features, including the presence of large coarse-grained phyllosilicate clasts, periclase, and unusual objects containing phyllosilicate, Fe-sulphide, periclase, phosphate and carbonate grains, are inconsistent with classification as CI chondrites.

Tomeoka (1990a, 1990b) reported that the abundance of coarse-grained phyllosilicate clasts is much higher in Y-82162 than in the CI chondrites, although Morlok et al. (2006) showed that the CI chondrites are breccias and the distribution of such clasts is highly variable. Tomeoka (1990a, 1990b) proposed that late-stage aqueous alteration degraded coarse-grained phyllosilicate clasts into finer-grained phyllosilicates and matrix materials. They suggested that coarse-grained

phyllosilicate clasts, plus phyllosilicate veins, were products of early stage alteration, and survived in Y-82162 as it avoided the later processing that occurred on the CI parent body. Iron sulphides are much more abundant in the matrix of Y-82162, Y-980115 and Y-86029 than the CI chondrites (Tomeoka et al., 1989a; Tonui et al., 2003), consistent with our XRD analyses, and implying that the availability of sulphur was much higher. Phosphates are also more common in Y-82162, Y-980115 and Y-86029 compared to CI chondrites, and may have formed contemporaneously with the coarse-grained phyllosilicates, magnetite and Fe-sulphides with which they are often associated (Tomeoka et al., 1989a; Tonui et al., 2003). Alternatively, the euhedral shape of the phosphate crystals possibly suggests formation from a melt following thermal metamorphism.

Large periclase clasts, such as those observed in Y-82162, Y-980115 and Y-86029 have not been found in other carbonaceous chondrite groups. Tonui et al. (2003) suggested that periclase in Y-86029 formed via thermal metamorphism and decomposition of Mg-Fe-rich carbonates such as magnesite and siderite. This is supported by the heating experiments of Nozaki et al. (2006), who showed that Mg-Fe-rich carbonates in aqueously altered meteorites decompose to magnesiowüstite at temperatures > 500 °C and pressures of 10^{-3} – 10^{-1} torr. Furthermore, Schofield et al. (2014) imaged the growth of crystallographically controlled skeletal magnetite lamellae in oxidised magnesiowüstite, textures that are observed in the Y-82162, Y-980115 and Y-86029 grains (Fig. 4; Tonui et al., 2003). However, the exact nature and formation mechanism of the large (up to ~700 μm) carbonate precursors is unclear. We suggest that they may have been similar to the large dolomite grain found by Fujiya et al. (2011, 2013) in Y-980115, which they speculated formed through replacement of a chondrule or CAI. Such grains would be analogous to the "Type 2″ carbonates observed in CM chondrites (Lee et al., 2014). Thermal decomposition of Mg-Fe-rich carbonates would have occurred at 500–800 °C (Tonui et al., 2003; Nozaki et al., 2006; King et al., 2015b), comparable to the estimated peak metamorphic temperatures for Y-82162, Y-980115 and Y-86029.

The most obvious difference between Y-82162, Y-980115 and Y-86029 and the CI chondrites is the objects consisting of phyllosilicate, Fe-sulphide, periclase and phosphate grains encased in dolomite. The objects are surrounded by FGRs and appear to be relict chondrules and CAIs. The CI chondrites contain abundant matrix and generally lack obvious chondrules and CAIs, although there have been reports of rare fully intact or fragments of refractory inclusions (e.g. Zolensky and Frank, 2014). Nevertheless, the unusual objects and FGRs are not found in the CI chondrites, indicating that Y-82162, Y-980115 and Y-86029 accreted different starting materials and were altered under different environmental conditions.

Polished sections of Y-86720, Y-86789 and B-7904 were not investigated in this study but are described in the literature; they contain abundant matrix, Fe-sulphides, carbonates, phosphates and metal (Tomeoka et al., 1989b; Akai, 1990; Tomeoka, 1990a; Bischoff and Metzler, 1991; Ikeda, 1992; Tonui et al., 2014). The matrix of these meteorites consists of dehydrated phyllosilicates and fine-grained olivine and pyroxene that recrystallized during thermal metamorphism at temperatures > 750 °C. Based on its mineralogy and textures it has been suggested that B-7904 was most closely related to the CM chondrites before the intense heating. For example, B-7904 contains (~20 vol %) chondrules that have undergone partial aqueous alteration, similar to those seen in CM2 chondrites (Bischoff and Metzler, 1991). Bischoff and Metzler (1991) reported that the mean diameter of chondrules in B-7904 is larger than typical CM chondrites, although Nakato et al. (2008) found them to be the same size. Bischoff and Metzler (1991) also estimated a CAI abundance in B-7904 of < 0.2 vol%, while Harries and Langenhorst (2013) attributed rare aggregates of Mg-Al spinel grains to relict CAIs in this meteorite.

Y-86720 and Y-86789 have a low abundance of chondrules, and these have been entirely replaced by phyllosilicates, comparable to the textures seen in CM1 chondrites (Tomeoka et al., 1989b; Bischoff and Metzler, 1991; Ikeda, 1992; Matsuoka et al., 1996). Possible pseudomorphs of CAIs have also been identified in Y-86720 (Tomeoka et al., 1989b). Like CM chondrites, the chondrules and pseudomorphs in Y-86720, Y-86789 and B-7904 are surrounded by FGRs, although they often appear "blurred or integrated" with the matrix due to annealing at high temperatures (Tonui et al., 2014). In addition, B-7904 has clasts with intimate mixtures of Fe-sulphides and dehydrated phyllosilicates that could be remnants of thermally decomposed tochilinite-cronstedtite intergrowths (TCIs), which are a common feature of CM chondrites (Nakamura, 2005).

Mineralogical differences between Y-86720, Y-86789 and B-7904 and the CM chondrites include the presence of metal and a low abundance of magnetite in the matrix. These can probably be attributed to the high peak metamorphic temperatures experienced by these meteorites. The abundance of Fe-sulphides and phosphates are also much higher in Y-86720, Y-86789 and B-7904; however the main difference between these meteorites and the CM chondrites is the composition of the matrix, which is a mixed serpentine/smectite (Tomeoka et al., 1989b; Akai, 1990; Tomeoka, 1990a; Bischoff and Metzler, 1991; Ikeda, 1992; Tonui et al., 2014), whereas it is predominantly serpentines in the CMs (Fig. 2; Zolensky et al., 1993). The composition of the matrix in Y-86720, Y-86789, and B-7904 overlaps with the CI chondrites, and Y-82162, Y-980115 and Y-86029 (Fig. 2 and Table 2).

We propose that based on their petrographic characteristics Y-82162, Y-980115, Y-86029, Y-86720, Y-86789 and B-7904 form a single group (the CYs) that is distinct from the CI and CM chondrites. The CYs all experienced aqueous alteration, the effects of which were later overprinted by thermal metamorphism. Evidence for a genetic relationship between the CYs includes the same matrix compositions, the availability of sulphur, and similar textures, such as partially to fully hydrated chondrules and pseudomorphs surrounded by FGRs. To our knowledge periclase has not been found in Y-86720 and Y-86789, and B-7904, which might reflect a low overall abundance of carbonates in these meteorites following aqueous alteration or preferential formation of metal rather than magnesiowüstite under reducing conditions during metamorphism at higher temperatures (Nozaki et al., 2006). We conclude that the CY chondrites were derived from the same starting materials and processed under generally similar conditions, but that variations in local factors on the parent body, such as temperature, pH, time and water/rock ratios, led to differences in both the degree of aqueous alteration and peak metamorphic temperatures recorded by these meteorites.

4.6. Parent body history of CY chondrites

The CY chondrite parent body accreted a mixture of chondrules and CAIs with FGRs, matrix and ices either in the outer regions of the main asteroid belt (~2 – 3 AU), or possibly even beyond the orbit of Jupiter (e.g. Warren, 2011). As the ices melted the resulting fluids reacted with anhydrous silicates to form a secondary mineral assemblage of phyllosilicates, oxides and carbonates. Fujiya et al. (2013) reported a Mn-Cr age of 4563.8 (± ~2) Ma for a single dolomite grain in Y-980115, consistent with the ages of carbonates in CI and CM chondrites (de Leuw et al., 2010; Fujiya et al., 2012). This suggests that aqueous alteration in the CY parent body was contemporaneous with the parent bodies of other aqueously altered carbonaceous chondrites. Mineralogy and oxygen isotopic compositions indicate that the CY chondrites are most similar to the CIs, for which Fujiya et al. (2013) calculated that the parent body accreted to > 100 km in diameter ~3 – 4 Myr after CAI formation and aqueous alteration lasted for ~10 Myr. However, the CY chondrites contain relict chondrules and CAIs, which are absent from the CIs, suggesting that the parent bodies must have formed in different reservoirs of the protoplanetary disk.

The CYs range from partially altered petrologic type 2 to fully hydrated type 1 chondrites. This variation in the degree of aqueous alteration is comparable to the CM chondrites, where it is attributed to

differences in either the duration of alteration, water/rock ratios, or the temperature under which hydration occurred. How long aqueous processes were active on the CY parent body is unknown because of the very limited chronological data currently available in the literature, but Mn-Cr ages for carbonates in the CM2 and CM1 chondrites suggest they were altered for similar periods of time (de Leuw et al., 2010; Fujiya et al., 2012). Variable water/rock ratios, caused by heterogeneous accretion of ices, transport of fluids along cracks (Rubin, 2012) or differential compaction (Alexander et al., 2013), should be reflected in bulk oxygen isotopic compositions (Clayton and Mayeda, 1999). The CY chondrites all have the same bulk oxygen isotopic compositions (Fig. 12) implying that alteration took place under the same water/rock ratios, although the effects of late stage thermal metamorphism also need to be considered.

Temperatures of aqueous alteration have been estimated at < 100 °C for the CM2 chondrites (DuFresne and Anders, 1962; Zolensky et al., 1989; Clayton and Mayeda, 1999; Baker et al., 2002), > 120 °C for the CM1s (Zolensky et al., 1997; King et al., 2017a), and from 50 to 150 °C for the CIs (Leshin et al., 1997; Clayton and Mayeda, 1999). Many researchers conclude that the source of heat required to melt accreted ices was radiogenic (i.e. decay of ^{26}Al), with the highest temperatures found either within the interior of a parent body, or potentially at near-surface regions due to convection (e.g. Palguta et al., 2010). However, there is also evidence that some aqueous alteration was related to impact heating, which would preferentially increase temperatures at the surface of a parent body (e.g. Lee and Nicholson, 2009; Rubin, 2012). For example, Lee et al. (2019) recently proposed a new model for the CM parent body whereby an early period of alkali-halogen metasomatism driven by impact heating was followed by low temperature aqueous alteration, either during post-impact cooling or later radiogenic heating. Based on observations of CI and CM chondrites, we suggest that the CYs were probably all aqueously altered at < 200 °C, but that the degree of hydration was controlled by regional temperature variations within the parent body.

In the CY chondrites the record of low temperature aqueous alteration has clearly been overprinted by the effects of thermal metamorphism. The peak metamorphic temperature during this late stage event was > 500 °C, high enough to dehydrate phyllosilicates and likely cause decomposition of carbonates (into periclase), which break down at 500–800 °C. The survival of dolomite in Y-980115 therefore suggests either that thermal metamorphism was heterogeneous, or that there was a period of aqueous alteration after the metamorphic event. We found a phyllosilicate vein cutting through a periclase clast, perhaps hinting at the latter scenario. However, as periclase is unstable in contact with H_2O at temperatures < 900 °C and reacts to form brucite (Williams et al., 1982), the vein must have formed after the carbonate precursor but before thermal metamorphism. Based on the survival of large periclase clasts we infer that phyllosilicates, and associated magnetite and carbonates, formed during early stage aqueous alteration, and that there was no further significant hydration of the CY chondrites after thermal metamorphism. This is also consistent with the relatively high abundance of coarse-grained phyllosilicate clasts in the CY chondrites.

The exact mechanism, timing and duration of post-hydration heating of aqueously altered carbonaceous chondrites remains poorly constrained. It has been estimated that B-7904 was heated on the order of hours to several years (Nakato et al., 2008), and short-lived heating is consistent with the structure of organic materials in other aqueously and thermally altered carbonaceous chondrites (e.g. Yabuta et al., 2010; Quirico et al., 2018). Qualitative comparison between the Fe-sulphide exsolution textures we find in Y-82162 and Y-980115 and those seen in artificially heated pyrrhotite also indicate brief heating (e.g. Kelly and Vaughan, 1983; Kimura et al., 2011). These timescales are inconsistent with radiogenic heating over millions of years and indicate that impacts or possibly solar radiation were the cause of thermal metamorphism (Nakamura, 2005). We favour impacts as they would produce the heterogeneous heating that we observe in the CY chondrites.

4.7. Terrestrial history of CY chondrites

An interesting feature of the CY chondrites is that most were recovered from the Yamato Mountain range in Antarctica. This may be a sampling bias or could be related to the young surface age of this collection site (~50% of meteorites have terrestrial ages of < 25,000 years, Jull et al., 1998) and changes in the meteoroid flux over time. Zolensky et al. (2005) suggested that because the CY chondrites have short CRE ages, young terrestrial ages (< 70,000 years), and were found on some of the youngest Antarctic surfaces, they may be derived from the break-up of a single Earth-crossing asteroid as little as ~200,000 years ago. We note that there are other CY candidates including two small (< 15 g) Antarctic meteorites, Y-86737 and Y-980134, that are currently classified as CIs, but also the hot desert finds Dhofar (Dho) 1988 ($C2_{ung}$) and Dho 2066 ($C2_{ung}$), which have oxygen isotopic compositions that fall within the CY field.

4.8. Relationship of CY chondrites to asteroids

Previous studies have shown that the visible and near-infrared (VNIR) reflectance spectra of the CY chondrites are very dark, flat and relatively featureless compared to the CIs and CMs (Hiroi et al., 1993, 1996; Cloutis et al., 2012; King et al., 2017b). The CY chondrites do show features in the 3 μm region– attributed to $-OH/H_2O$ bonds – but these are weak relative to those observed for the CIs and CMs (e.g. Osawa et al., 2005; King et al., 2017b). These characteristics can all be related to the dehydration and dehydroxylation of the phyllosilicates and possible shock darkening induced by impact heating (e.g. Sugita et al., 2019).

The Hayabusa2 mission is currently investigating the near-Earth C-type asteroid Ryugu, with the aim of returning samples back to Earth in 2020. Prior to arrival Ryugu was linked to the CI and CM chondrites, with tentative evidence for partial dehydration of the surface (Vilas, 2008; Moskovitz et al., 2013; Perna et al., 2017; Le Corre et al., 2018). The preliminary survey conducted by Hayabusa2 indicates a homogenous surface with flat VNIR spectra and only a weak feature at 2.72 μm from Mg – OH in Mg-rich phyllosilicates (Kitazato et al., 2019). The surface of Ryugu is much darker than the CI and CM chondrites, and the closest spectral match in the meteorite collection is the highly

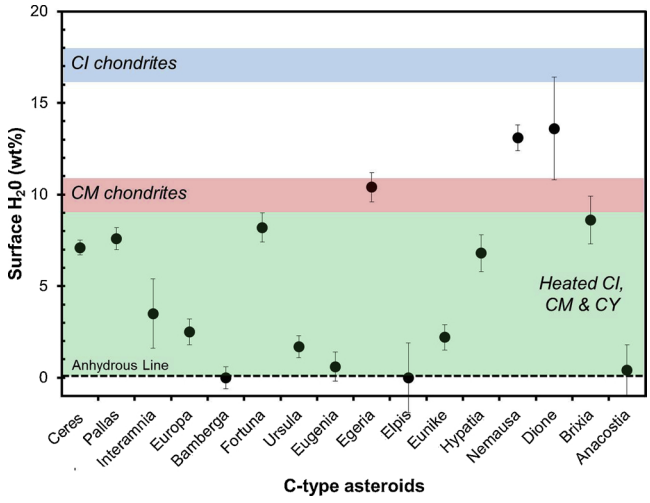

Fig. 14. Estimated H_2O abundances for C-type asteroid surfaces compared to unheated and heated CI, CM and CY carbonaceous chondrites. Asteroid data are from Rivkin et al. (2003), and meteorite data are from Alexander et al. (2013); Garenne et al. (2014), and King et al. (2015b).

aqueously altered and thermally metamorphosed carbonaceous chondrites (Kitazato et al., 2019; Sugita et al., 2019). Although terrestrial and space weathering effects need to be taken into account, we suggest that the CY chondrites are the best analogues for materials on the surface of Ryugu. This is in agreement with the hypothesis that Ryugu is a rubble-pile asteroid that formed through collisional events and therefore should record a history of impact heating (Sugita et al., 2019; Watanabe et al., 2019).

A significant fraction of C-type asteroids appear to have dehydrated surfaces with VNIR spectral features comparable to the CY chondrites (Hiroi et al., 1993, 1996). Furthermore, the surface H_2O abundances of C-type asteroids estimated using the 3 μm regionare in good agreement with those in the CY chondrites (Fig. 14; Rivkin et al., 2003). It therefore seems likely that CY-like materials are widespread throughout the solar system, although whether they are distributed according to asteroid sizes, distances from the Sun, or orbital and geological evolution is an open question.

5. Summary

We have combined new mineralogical, petrographic, and noble gas analyses with literature data to understand the alteration history of the carbonaceous chondrites Y-82162, Y-980115, Y-86029, Y-86720, Y-86789 and B-7904. We show that these meteorites experienced varying degrees of aqueous alteration, the effects of which were later overprinted by post-hydration thermal metamorphism at temperatures of > 500 °C. Evidence for thermal metamorphism includes the presence of dehydrated phyllosilicates, recrystallized silicates and melted Fe-sulphides, and depletions in H_2O, volatile trace element and noble gas abundances. We suggest that based on similar mineralogy, textures, and chemical characteristics these meteorites are genetically related, and differ from other carbonaceous chondrites in the following respects:-

- they have distinct bulk oxygen isotopic compositions of $\delta^{17}O$ ~12‰ and $\delta^{18}O$ ~22‰. These compositions are the heaviest recorded in any meteorite group and are consistent with modification by intense periods of parent body aqueous alteration and thermal metamorphism.
- their abundance of Fe-sulphide (~10 – 30 vol%) is considerably higher than in the aqueously altered CI and CM chondrites (< 5 vol %), implying that sulphur was more readily available on the parent body. Phosphates are also more common in these meteorites.
- they contain periclase, and unusual objects consisting of phyllosilicates, Fe-sulphides, periclase, phosphates and carbonates that have not been found in other carbonaceous chondrites. Periclase likely formed through the decomposition of large Mg-Fe-rich carbonates precursors, and the objects are surrounded by fine-grained rims and may be relict chondrules and/or CAIs.

We suggest that these features cannot be entirely attributed to parent body processes, and therefore recommend that Y-82162, Y-980115, Y-86029, Y-86720, Y-86789 and B-7904 should be considered a new carbonaceous chondrite group. We support the original suggestion of Ikeda (1992) that this be called the CY ("Yamato-type") group. The CY chondrites have short CRE ages (≤1.3 Ma) consistent with a near-Earth source, and remote observations by the Hayabusa2 spacecraft indicate that the near-Earth rubble-pile asteroid Ryugu is a possible parent body.

Acknowledgements

We would like to thank the National Institute of Polar Research (NIPR), Japan, for providing the samples investigated in this study. Jens Najorka, John Spratt and Tobias Salge are thanked for assistance with the XRD and SEM data collection and analysis, and Andy Rivkin is thanked for providing the asteroid data. We thank Kazushige Tomeoka and Mike Zolensky for detailed reviews that improved this manuscript and Falko Langenhorst for editorial handling. This work was funded by the Science and Technology Facilities Council (STFC), UK, through grants ST/R000727/1 (AJK, PFS and SSR) and 1860431 (HCB), and supported by the Swiss NSF (DK) and the NCCR "Planet S", funded by the Swiss SNF (HB).

Appendix A

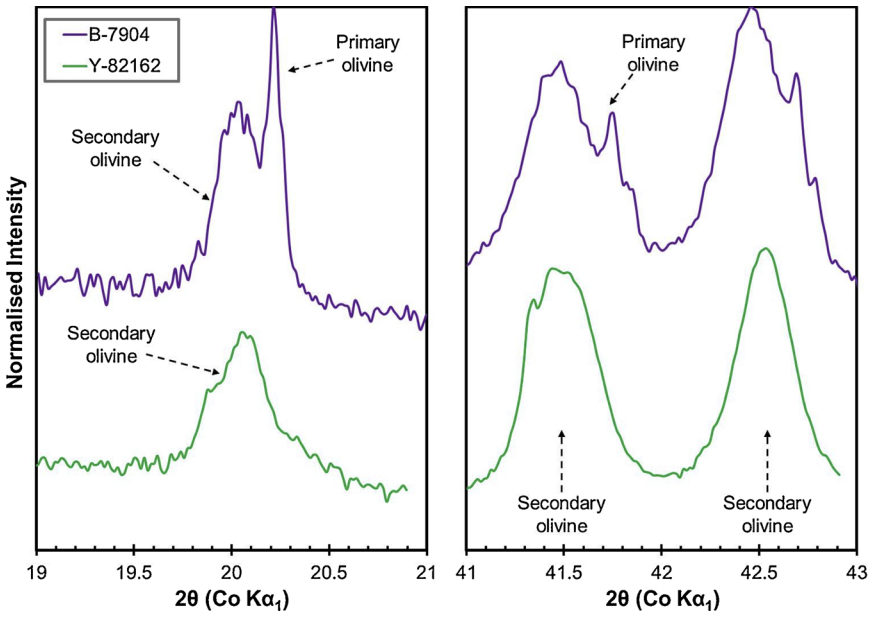

Fig. A1. XRD patterns highlighting the presence of crystalline primary olivine in B-7904. The patterns were collected using a PANalytical X'Pert Pro scanning XRD and Co $K\alpha_1$ radiation.

Table A1
Element abundances in wt% for bulk CI/CY chondrites used to determine cosmogenic $^{20}Ne/^{22}Ne$ and $^{21}Ne/^{22}Ne$ isotope ratios and $^{21}Ne_{cos}$ production rates with the model predictions by Leya and Masarik (2009).

	CI mean[(a)]	Y-980115[(b)]	Y-82162[(c)]	Y-86720[(c)]	B-7904[(c)]
C	3.52	–	–	–	–
N	0.29	–	–	–	–
O	45.82	40.80	39.79	38.48	36.90
Na	0.50	0.58	0.65	0.49	0.49
Mg	9.59	10.59	12.18	13.70	14.30
Al	0.85	0.91	1.20	2.03	1.75
Si	10.65	17.07*	12.62	14.35	14.72
S	5.41	6.20	7.32	4.82	4.18
Ca	0.91	1.01	1.46	1.44	1.59
K	0.05	0.06	0.11	0.03	0.03
Ti	0.04	0.05	0.14	0.05	0.10
Mn	0.19	0.21	0.24	0.14	0.19
Fe	18.28	21.28	22.81	23.16	24.30
Ni	1.06	1.26	1.01	0.91	0.95
Rb	0.00021	0.00026	–	–	–
Sr	0.00077	–	–	–	–
Y	0.00015	–	–	–	–
Zr	0.00040	0.00039	–	–	–
Ba	0.00023	0.00026	–	–	–
Te	0.00023	0.00030	–	–	–

References: (a) McSween and Huss (2010), (b) Braukmüller et al. (2018), and (c) Ikeda (1992). *derived from SiO_2 [wt%] = 100 - SUM(major oxide abundances [wt %]) by converting major element into corresponding oxide abundances, assuming H_2O = 7.5 wt% (see main text).

References

Akai, J., 1990. Mineralogical evidence of heating events in Antarctic carbonaceous chondrites, Y-86720 and Y-82162. Proc. NIPR Symp. Antarct. Meteorites 3, 55–68.
Alexander, C.M.O.'D., Bowden, R., Fogel, M.L., Howard, K.T., Herd, C.D.K., Nittler, L.R., 2012. The provenances of asteroids, and their contributions to the volatile inventories of the terrestrial planets. Science 337, 721–723.
Alexander, C.M.O.'D., Howard, K.T., Bowden, R., Fogel, M.L., 2013. The classification of CM and CR chondrites using bulk H, C and N abundances and isotopic compositions. Geochim. Cosmochim. Acta 123, 244–260.
Amari, S., Lewis, R.S., Anders, E., 1995. Interstellar grains in meteorites: III. Graphite and its noble gases. Geochim. Cosmochim. Acta 59, 1411–1426.
Baker, L., Franchi, I.A., Wright, I.P., Pillinger, C.T., 2002. The oxygen isotopic composition of water from Tagish Lake: its relationship to low-temperature phases and to other carbonaceous chondrites. Meteorit. Planet. Sci. 37, 977–985.
Barrat, J.-A., Zanda, B., Moynier, F., Bollinger, C., Liorzou, C., Bayon, G., 2012. Geochemistry of CI chondrites: major and trace elements, and Cu and Zn isotopes. Geochim. Cosmochim. Acta 83, 79–92.
Bischoff, A., Metzler, K., 1991. Mineralogy and petrography of the anomalouscarbonaceous chondrites Yamato-86720, Yamato-82162, and Belgica-7904. Proc. NIPR Symp. Antarct. Meteorites 4, 226–246.
Bland, P.A., Cressey, G., Menzies, O.N., 2004. Modal mineralogy of carbonaceous chondrites by X-ray diffraction and Mössbauer spectroscopy. Meteorit. Planet. Sci. 39, 3–16.
Braukmüller, N., Wombacher, F., Hezel, D.C., Escoube, R., Münker, C., 2018. The chemical composition of carbonaceous chondrites: implications for volatile element depletion, complementarity and alteration. Geochim. Cosmochim. Acta 239, 17–48.
Brearley, A.J., 2006. The action of water. In: Lauretta, D.S., McSween, H.Y. (Eds.), Meteorites and the Early Solar System II, pp. 587–624.
Brearley, A.J., Jones, R.H., 1998. Chondritic meteorites. Rev. Mineral. Geochem. 36, 31–398.
Busemann, H., Baur, H., Wieler, R., 2000. Primordial noble gases in "phase Q" in carbonaceous chondrite and ordinary chondrites studied by closed-system stepped etching. Meteorit. Planet. Sci. 35, 949–973.
Clayton, R.N., Mayeda, T.K., 1999. Oxygen isotope studies of carbonaceous chondrites. Geochim. Cosmochim. Acta 63, 2089–2104.
Clayton, R.N., Mayeda, T.K., 2009. Kinetic isotope effects in oxygen in the laboratory dehydration of magnesian minerals. J. Phys. Chem. 113, 2212–2217.
Clayton, R.N., Mayeda, T.K., Hiroi, T., Zolensky, M.E., Lipschutz, M.E., 1997. Oxygen isotopes in laboratory-heated CI and CM chondrites (abstract). Meteorit. Planet. Sci. 32, 30.
Cloutis, E.A., Hudon, P., Hiroi, T., Gaffey, M.J., 2012. Spectral reflectance properties of carbonaceous chondrites 4: aqueously altered and thermally metamorphosed meteorites. Icarus 220, 586–617.
Cressey, G., Schofield, P.F., 1996. Rapid whole-pattern profile stripping method for the quantification of multiphase samples. Powder Diffr. 11, 35–39.
de Leuw, S., Rubin, A.E., Wasson, J.T., 2010. Carbonates in CM chondrites: complex formational histories and comparison to carbonates in CI chondrites. Meteorit. Planet. Sci. 45, 513–530.
DuFresne, E.R., Anders, E., 1962. On the chemical evolution of the carbonaceous chondrites. Geochim. Cosmochim. Acta 26, 1085–1114.
Ebihara, M., Shinonaga, T., 1989. Chemical compositions of some primitive carbonaceous chondrites from Antarctica. Papers Presented to the 14th Symposium on Antarctic Meteorites 35.
Endress, M., Bischoff, A., 1996. Carbonates in CI chondrites: clues to parent body evolution. Geochim. Cosmochim. Acta 60, 489–507.
Eugster, O., 2003. Cosmic-ray exposure ages of meteorites and lunar rocks and their significance. Chem. Erde 63, 3–30.
Friedrich, J.M., Abreu, N.M., Wolf, S.F., Troiano, J.M., Stanek, G.L., 2018. Redux-influenced trace element compositional differences among variably aqueously altered CM chondrites. Geochim. Cosmochim. Acta 237, 1–17.
Fujiya, W., Sugiura, N., Sano, Y., 2011. Alteration history in the CI chondrite parent body inferred from Mn-Cr dating of carbonates (abstract). Meteorit. Planet. Sci. 46, 5240.
Fujiya, W., Sugiura, N., Hotta, H., Ichimura, K., Sano, Y., 2012. Evidence for the late formation of hydrous asteroids from young meteoritic carbonates. Nature Comm. 3, 627.
Fujiya, W., Sugiura, N., Sano, Y., Hiyagon, H., 2013. Mn-Cr ages of dolomites in CI chondrites and the Tagish Lake ungrouped carbonaceous chondrite. Earth. Plan. Sci. Lett. 362, 130–142.
Garenne, A., Beck, P., Montes-Hernandez, G., Chirac, R., Toche, F., Quirico, E., Bonal, L., Schmitt, B., 2014. The abundance and stability of "water" in type 1 and 2 carbonaceous chondrites (CI, CM and CR). Geochim. Cosmochim. Acta 137, 93–112.
Hanowski, N.P., Brearley, A.J., 2001. Aqueous alteration of chondrules in the CM carbonaceous chondrite Allan Hills 81002: implications for parent body alteration. Geochim. Cosmochim. Acta 65, 495–518.
Haramura, H., Kushiro, I., Yanai, K., 1983. Chemical compositions of Antarctic meteorites. I. Mem. Natl Inst. Polar Res. Spec. (30), 109–121.
Harries, D., Langenhorst, F., 2013. The nanoscale mineralogy of Fe,Ni sulphides in pristine and metamorphosed CM and CM/CI-like chondrites: tapping a petrogenetic record. Meteorit. Planet. Sci. 48, 879–903.
Heber, V.S., Wieler, R., Baur, H., Olinger, C., Friedmann, T.A., Burnett, D.S., 2009. Noble gas composition of the solar wind as collected by the Genesis mission. Geochim. Cosmochim. Acta 73, 7414–7432.
Herzog, G.F., Caffee, M., 2014. Cosmic-ray exposure ages of meteorites. In: 2nd ed. In: Davies, A.M. (Ed.), Treatise on Geochemistry Vol. 2. Planets, Asteroids, Comets and the Solar System, pp. 419–453.
Hiroi, T., Pieters, C.M., Zolensky, M.E., Lipschutz, M.E., 1993. Evidence of thermal metamorphism on C, G, B, and F asteroids. Science 261, 1016–1018.
Hiroi, T., Pieters, C.M., Zolensky, M.E., Lipschutz, M.E., 1996. Thermal metamorphism of the C, G, B, and F asteroids seen from the 0.7-μm, 3-μm, and UV absorption strengths in comparison with carbonaceous chondrites. Meteorit. Planet. Sci. 31, 321–327.
Howard, K.T., Benedix, G.K., Bland, P.A., Cressey, G., 2009. Modal mineralogy of CM2 chondrites by X-ray diffraction (PSD-XRD). Part 1: total phyllosilicate abundance and the degree of aqueous alteration. Geochim. Cosmochim. Acta 73, 4576–4589.
Howard, K.T., Benedix, G.K., Bland, P.A., Cressey, G., 2011. Modal mineralogy of CM chondrites by X-ray diffraction (PSD-XRD). Part 2: degree, nature and settings of aqueous alteration. Geochim. Cosmochim. Acta 75, 2735–2751.
Howard, K.T., Alexander, C.M.O.'D., Schrader, D.L., Dyl, K.A., 2015. Classification of hydrous meteorites (CR, CM and C2 ungrouped) by phyllosilicate fraction: PSD-XRD modal mineralogy and planetesimal environments. Geochim. Cosmochim. Acta 149, 206–222.
Huss, G.R., Lewis, R.S., 1994. Noble gases in presolar diamonds I: three distinct components and their implications for diamond origins. Meteoritics 29, 791–810.
Ikeda, Y., 1991. Petrology and mineralogy of the Yamato-82162 chondrite (CI). Proc. NIPR Symp. Antarct. Meteorites 4, 187–225.
Ikeda, Y., 1992. An overview of the research consortium, "Antarctic carbonaceous chondrites with CI affinities, Yamato-86720, Yamato-82162, and Belgica-7904. Proc. NIPR Symp. Antarct. Meteorites 5, 49–73.
Jull, A.J.T., Cloudt, S., Cielaszyk, E., 1998. ^{14}C terrestrial ages of meteorites from Victoria

Land, Antarctica, and the infall rates of meteorites. In: Grady, M.M., Hutchison, R., McCall, G.J.H., Rothery, D.A. (Eds.), Meteorites: Flux With Time and Impact Effects, pp. 75–92.
Kallemeyn, G.W., 1988. Compositional study of carbonaceous chondrites with CI-CM affinities. Papers Presented to the 13th Symposium on Antarctic Meteorites 132–134.
Kallemeyn, G.W., Wasson, J.T., 1981. The compositional classification of chondrites – I. The carbonaceous chondrite groups. Geochim. Cosmochim. Acta 45, 1217–1230.
Kelly, D.P., Vaughan, D.J., 1983. Pyrrhotine-pentlandite ore textures: a mechanistic approach. Min. Mag. 47, 453–463.
Kimura, M., Grossman, J.N., Weisberg, M.K., 2011. Fe-Ni metal and sulfide minerals in CM chondrites: an indicator for thermal history. Meteorit. Planet. Sci. 46, 431–442.
King, A.J., Schofield, P.F., Howard, K.T., Russell, S.S., 2015a. The modal mineralogy of CI and CI-like chondrites by X-ray diffraction. Geochim. Cosmochim. Acta 165, 148–160.
King, A.J., Solomon, J.R., Schofield, P.F., Russell, S.S., 2015b. Characterising the CI and CI-like carbonaceous chondrites using thermogravimetric analysis and infrared spectroscopy. Earth Planets Space 67, 198.
King, A.J., Schofield, P.F., Russell, S.S., 2017a. Type 1 aqueous alteration in CM carbonaceous chondrites: implications for the evolution of water-rich asteroids. Meteorit. Planet. Sci. 52, 1197–1215.
King, A.J., Maturilli, A., Schofield, P.F., Helbert, J., Russell, S.S., 2017b. The thermal history of CI and CM chondrites and their relationship to primitive asteroid surfaces. Meteorit. Planet. Sci. (abstract) 52, 6220.
Kitazato, K., Milliken, R.E., Iwata, T., Abe, M., Ohtake, M., Matsuura, S., Arai, T., Nakauchi, T., Nakamura, T., Matsuoka, M., Senshu, H., Hirata, N., Hiroi, T., Pilorget, C., Brunetto, R., Poulet, F., Riu, L., Bibring, J.-P., Takir, D., Domingue, D.L., Vilas, F., Barucci, M.A., Perna, D., Palomba, E., Galiano, A., Tsumura, K., Osawa, T., Komatsu, M., Nakato, A., Arai, T., Takato, N., Matsunaga, T., Takagi, Y., Matsumoto, K., Kouyama, T., Yokota, Y., Tatsumi, E., Sakatani, N., Yamamoto, Y., Okada, T., Sugita, S., Honda, R., Morota, T., Kameda, S., Sawada, H., Honda, C., Yamada, M., Suzuki, H., Yoshioka, K., Hayakawa, M., Ogawa, K., Cho, Y., Shirai, K., Shimaki, Y., Hirata, N., Yamaguchi, A., Ogawa, N., Terui, F., Yamaguchi, T., Takei, Y., Saiki, T., Nakazawa, S., Tanaka, S., Yoshikawa, M., Watanabe, S., Tsuda, Y., 2019. The surface composition of asteroid 162173 Ryugu from Hayabusa2 near-infrared spectroscopy. Science 364, 272–275.
Krietsch, D., Busemann, H., Riebe, M.E.I., King, A.J., Maden, C., 2019. Complete characterisation of the noble gas inventory in CR chondrite Miller Range 090657 by direct etch release. Meteorit. Planet. Sci. (abstract) 54.
Le Corre, L., Sanchez, J.A., Reddy, V., Takir, D., Cloutis, E.A., Thirouin, A., Becker, K.J., Li, J.-Y., Sugita, S., Tatsumi, E., 2018. Ground-based characterisation of Hayabusa2 mission target asteroid 162173 Ryugu: constraining mineralogical composition in preparation for spacecraft operations. Mon. Not. R. Astron. Soc. 475, 614–623.
Lee, M.R., Nicholson, K., 2009. Ca-carbonate in the Orgueil (CI) carbonaceous chondrite: mineralogy, microstructure and implications for parent body history. Earth. Plan. Sci. Lett. 280, 268–275.
Lee, M.R., Lindgren, P., Sofe, M.R., 2014. Aragonite, breunnerite, calcite and dolomite in the CM carbonaceous chondrites: high fidelity recorders of progressive parent body aqueous alteration. Geochim. Cosmochim. Acta 144, 126–156.
Lee, M.R., Cohen, B.E., King, A.J., 2019. Alkali-halogen metasomatism of the CM carbonaceous chondrites. Meteorit. Planet. Sci (in review).
Leshin, L.A., Rubin, A.E., McKeegan, K.D., 1997. The oxygen isotopic composition of olivine and pyroxene from CI chondrites. Geochim. Cosmochim. Acta 61, 835–845.
Lewis, R.S., Amari, S., Anders, E., 1994. Interstellar grains in meteorites: II. SiC and its noble gases. Geochim. Cosmochim. Acta 58, 471–494.
Leya, I., Masarik, J., 2009. Cosmogenic nuclides in stony meteorites revisited. Meteorit. Planet. Sci. 44, 1061–1086.
Matsuoka, K., Nakamura, T., Nakamuta, Y., Takaoka, N., 1996. Yamato-86789: a heated CM-like carbonaceous chondrite. Proc. NIPR Symp. Antarct. Meteorites 9, 20–36.
McSween Jr., H.Y., Huss, G.R., 2010. Cosmochemistry. Cambridge University Press.
Morlok, A., Bischoff, A., Stephan, T., Floss, C., Zinner, E., Jessberger, E.K., 2006. Brecciation and chemical heterogeneities of CI chondrites. Geochim. Cosmochim. Acta 70, 5371–5394.
Moskovitz, N.A., Abe, S., Pan, K.-S., Osip, D.J., Pefkou, D., Melita, M.D., Elias, M., Kitazato, K., Bus, S.J., DeMeo, F.E., Binzel, R.P., Abell, P.A., 2013. Rotational characterisation of Hayabusa II target asteroid (162173) 1999 JU3. Icarus 224, 24–31.
Nagao, K., Inoue, K., Ogata, K., 1984. Primordial rare gases in Belgica-7904 (C2) carbonaceous chondrite. Proc. NIPR Symp. Antarct. Meteorites 35, 257–266.
Nakato, A., Nakamura, T., Kitajima, F., Noguchi, T., 2008. Evaluation of dehydration mechanism during heating of hydrous asteroids based on mineralogical and chemical analysis of naturally and experimentally heated CM chondrites. Earth Planets Space 60, 855–864.
Nakamura, T., 2005. Post-hydration thermal metamorphism of carbonaceous chondrites. J. Mineral. Petrol. Sci. 100, 260–272.
Nozaki, W., Nakamura, T., Noguchi, T., 2006. Bulk mineralogical changes during heating in the upper atmosphere at temperatures below 1000°C. Meteorit. Planet. Sci. 41, 1095–1114.
Osawa, T., Kagi, H., Nakamura, T., Noguchi, T., 2005. Infrared spectroscopic taxonomy for carbonaceous chondrites from speciation of hydrous components. Meteorit. Planet. Sci. 40, 71–86.
Palguta, J., Schubert, G., Travis, B.J., 2010. Fluid flow and chemical alteration in carbonaceous chondrite parent bodies. Earth. Plan. Sci. Lett. 296, 235–243.
Paul, R.L., Lipschutz, M.E., 1990. Consortium study of labile trace elements in some Antarctic carbonaceous chondrites: antarctic and non-Antarctic meteorite comparisons. Proc. NIPR Symp. Antarct. Meteorites 3, 80–95.
Perna, D., Barucci, M.A., Ishiguro, M., Alvarez-Candal, A., Kuroda, D., Yoshikawa, M., Kim, M.-J., Fornasier, S., Hasegawa, S., Roh, D.-G., Müller, T.G., Kim, Y., 2017. Spectral and rotational properties of near-Earth asteroid (162173) Ryugu, target of the Hayabusa2 sample return mission. Astron. Astrophys. 599, L1.
Quirico, E., Bonal, L., Beck, P., Alexander, C.M.O.'D., Yabuta, H., Nakamura, T., Nakato, A., Flandinet, L., Montagnac, G., Schmitt-Kopplin, P., Herd, C.D.K., 2018. Prevalence and nature of heating processes in CM and C2-ungrouped chondrites as revealed by insoluble organic matter. Geochim. Cosmochim. Acta 241, 17–37.
Riebe, M.E.I., Welten, K.C., Meier, M.M.M., Wieler, R., Barth, M.I.F., Ward, D., Laubenstein, M., Bischoff, A., Caffee, M.W., Nishiizumi, K., Busemann, H., 2017a. Cosmic-ray exposure ages of six chondritic Almahata Sitta fragments. Meteorit. Planet. Sci. 52, 2353–2374.
Riebe, M.E., Busemann, H., Wieler, R., Maden, C., 2017b. Closed system step etching of CI chondrite Ivuna reveals primordial noble gases in the HF-solubles. Geochim. Cosmochim. Acta 205, 65–83.
Rivkin, A.S., Davies, J.K., Johnson, J.R., Ellison, S.L., Trilling, D.E., Brown, R.H., Lebofsky, L.A., 2003. Hydrogen concentrations on C-class asteroids derived from remote sensing. Meteorit. Planet. Sci. 38, 1383–1398.
Rubin, A.E., 2012. Collisional facilitation of aqueous alteration in CM and CV carbonaceous chondrites. Geochim. Cosmochim. Acta 90, 181–194.
Schofield, P.F., Smith, A.D., Scholl, A., Doran, A., Covey-Crump, S.J., Young, A.T., Ohldag, H., 2014. Chemical and oxidation-state imaging of mineralogical intergrowths: the application of X-ray photo-emission electron microscopy (XPEEM). Coord. Chem. Rev. 277–278, 31–43.
Sugita, S., Honda, R., Morota, T., Kameda, S., Sawada, H., Tatsumi, E., Yamada, M., Honda, C., Yokota, Y., Kouyama, T., Sakatani, N., Ogawa, K., Suzuki, H., Okada, T., Namiki, N., Tanaka, S., Iikima, Y., Yoshioka, K., Hayakawa, M., Cho, Y., Matsuoka, M., Hirata, N., Hirata, N., Miyamoto, H., Domingue, D., Hirabayashi, M., Nakamura, T., Hiroi, T., Michikami, T., Michel, P., Ballouz, R.-L., Barnouin, O.S., Ernst, C.M., Schröder, S.E., Kikuchi, H., Hemmi, R., Komatsu, G., Fukuhara, T., Taguchi, M., Arai, T., Senshu, H., Demura, H., Ogawa, Y., Shimaki, Y., Sekiguchi, T., Müller, T.G., Hagermann, A., Mizuno, T., Noda, H., Matsumoto, K., Yamada, R., Ishihara, Y., Ikeda, H., Araki, H., Yamamoto, K., Abe, S., Yoshida, F., Higuchi, A., Sasaki, S., Oshigami, S., Tsuruta, S., Asari, K., Tazawa, S., Shizugami, M., Kimura, J., Otsubo, T., Yabuta, H., Hasegawa, S., Ishiguro, M., Tachibana, S., Palmer, E., Gaskell, R., Le Corre, L., Jaumann, R., Otto, K., Schmitz, N., Abell, P.A., Barucci, M.A., Zolensky, M.E., Vilas, F., Thuillet, F., Sugimoto, C., Takaki, N., Suzuki, Y., Kamiyoshihara, H., Okada, M., Nagata, K., Fujimoto, M., Yoshikawa, Y., Yamamoto, Y., Shirai, K., Noguchi, R., Ogawa, N., Terui, F., Kikuchi, S., Yamaguchi, T., Oki, Y., Takao, Y., Takeuchi, H., Ono, G., Mimasu, Y., Yoshikawa, K., Takahashi, T., Takei, Y., Fujii, A., Hirose, C., Nakazawa, S., Hosoda, S., Mori, O., Shimada, T., Soldini, S., Iwata, T., Abe, M., Yano, H., Tsukizaki, R., Ozaki, M., Nishiyama, K., Saiki, T., Watanabe, S., Tsuda, Y., 2019. The geomorphology, color, and thermal properties of Ryugu: implications for parent-body processes. Science 364 eaaw0422.
Tomeoka, K., 1990a. Mineralogy and petrology of Belgica-7904: a new kind of carbonaceous chondrite from Antarctica. Proc. NIPR Symp. Antarct. Meteorites 3, 40–54.
Tomeoka, K., 1990b. Phyllosilicate veins in a CI meteorite: evidence for aqueous alteration on the parent body. Nature 345, 138–140.
Tomeoka, K., Kojima, H., Yanai, K., 1989a. Yamato-82162: a new kind of CI carbonaceous chondrite found in Antarctica. Proc. NIPR Symp. Antarct. Meteorites 2, 36–54.
Tomeoka, K., Kojima, H., Yanai, K., 1989b. Yamato-86720: a CM carbonaceous chondrite having experienced extensive aqueous alteration and thermal metamorphism. Proc. NIPR Symp. Antarct. Meteorites 2, 55–74.
Tonui, E.K., Zolensky, M.E., Lipschutz, M.E., Wang, M.-S., Nakamura, T., 2003. Yamato 86029: aqueously altered and thermally metamorphosed CI-like chondrite with unusual texture. Meteorit. Planet. Sci. 38, 269–292.
Tonui, E.K., Zolensky, M.E., Hiroi, T., Nakamura, T., Lipschutz, M.E., Wang, M.-S., Okudaira, K., 2014. Petrographic, chemical and spectroscopic evidence for thermal metamorphism in carbonaceous chondrites I: CI and CM chondrites. Geochim. Cosmochim. Acta 126, 284–306.
Trigo-Rodriguez, J.M., Rubin, A.E., Wasson, J.T., 2006. Non-nebular origin of dark mantles around chondrules and inclusions in CM chondrites. Geochim. Cosmochim. Acta 70, 1271–1290.
Valley, J.W., 1986. Stable isotope geochemistry in metamorphic rocks. In: Valley, J.W., Taylor, H.P., O'Neal, J.R. (Eds.), Stable Isotopes in High Temperature Geological Processes, pp. 445–489 Miner. Soc. Am. Rev. Miner. vol. 16.
Velbel, M.A., Tonui, E.K., Zolensky, M.E., 2012. Replacement of olivine by serpentine in the carbonaceous chondrite Nogoya (CM2). Geochim. Cosmochim. Acta 87, 117–135.
Velbel, M.A., Tonui, E.K., Zolensky, M.E., 2015. Replacement of olivine by serpentine in the Queen Alexandra Range 93005 carbonaceous chondrite (CM2): reactant-product compositional relations, and isovolumetric constraints on reaction stoichiometry and elemental mobility during aqueous alteration. Geochim. Cosmochim. Acta 148, 402–425.
Vilas, F., 2008. Spectral characterisitcs of Hayabusa 2 near-Earth asteroid targets 162173 1999 JU3 and 2001 QC34. Astron. J. 135, 1101–1105.
Warren, P.H., 2011. Stable-isotopic anomalies and the accretionary assemblage of the Earth and Mars: a subordinate role for carbonaceous chondrites. Earth. Plan. Sci. Lett. 311, 93–100.
Watanabe, S., Hirabayashi, M., Hirata, N., Hirata, N., Noguchi, R., Shimaki, Y., Ikeda, H., Tatsumi, E., Yoshikawa, M., Kikuchi, S., Yabuta, H., Nakamura, T., Tachibana, S., Ishihara, Y., Morota, T., Kitazato, K., Sakatani, N., Matsumoto, K., Wada, K., Senshu, H., Honda, C., Michikami, T., Takeuchi, H., Kouyama, T., Honda, R., Kameda, S., Fuse, T., Miyamoto, H., Komatsu, G., Sugita, S., Okada, T., Namiki, N., Arakawa, M., Ishiguro, M., Abe, M., Gaskell, R., Palmer, E., Barnouin, O.S., Michel, P., French, A.S., McMahon, J.W., Scheeres, D.J., Abell, P.A., Yamamoto, Y., Tanaka, S., Shirai, K., Matsuoka, M., Yamada, M., Yokota, Y., Suzuki, H., Yoshikawa, K., Takahashi, T., Takei, Y., Fujii, A., Hirose, C., Iwata, T., Hayakawa, M., Hosoda, S., Mori, O., Sawada, H., Shimada, T., Soldini, S., Yano, H., Tsukizaki, R., Ozaki, M., Iijima, Y., Ogawa, K., Fujimoto, M., Ho, T.-M., Moussi, A., Jaumann, R., Bibring, J.-P., Krause, C., Terui, F., Saiki, T., Nakazawa, S., Tsuda, Y., 2019. Hayabusa2 arrives at the carbonaceous asteroid 162173 Ryugu – a spinning top-shaped rubble pile. Science 364, 268–272.
Weber, H.W., Schultz, L., 1991. Noble gases in eight unusual carbonaceous chondrites (abstract). Meteoritics 26, 406.
Weisberg, M.K., McCoy, T.J., Krot, A.N., 2006. Systematics and evaluation of meteorite classification. In: Lauretta, D.S., McSween, H.Y. (Eds.), Meteorites and the Early Solar System II, pp. 19–52.

Wieler, R., 2002. Cosmic-ray-produced noble gases in meteorites. Rev. Mineral. Geochem. 47, 125–170.
Williams, H., Turner, F.J., Gilbert, C.M., 1982. Petrography: an Introduction to the Study of Rocks in Thin Sections, 2nd edition. W. H. Freeman and Company, San Francisco.
Yabuta, H., Alexander, C.M.O.'D., Fogel, M.L., Kilcoyne, A.L.D., Cody, G.D., 2010. A molecular and isotopic study of the macromolecular organic matter of the ungrouped C2 WIS 91600 and its relationship to Tagish Lake and PCA 91008. Meteorit. Planet. Sci. 45, 1446–1460.
Zolensky, M.E., Frank, D., 2014. Surviving high-temperature components in CI chondrites. Meteorit. Planet. Sci. (abstract) 49, 5202.
Zolensky, M.E., Bourcier, W.L., Gooding, J.L., 1989. Aqueous alteration on the hydrous asteroids: results of EQ3/6 computer simulations. Icarus 78, 411–425.
Zolensky, M.E., Barrett, R., Browning, L., 1993. Mineralogy and composition of matrix and chondrule rims in carbonaceous chondrites. Geochim. Cosmochim. Acta 57, 3123–3148.
Zolensky, M.E., Mittlefehldt, D.W., Lipschutz, M.E., Wang, M.-S., Clayton, R.N., Mayeda, T.K., Grady, M.N., Pillinger, C., Barber, D., 1997. CM chondrites exhibit the complete petrologic range from type 2 to 1. Geochim. Cosmochim. Acta 61, 5099–5115.
Zolensky, M.E., Abell, P., Tonui, E.K., 2005. Metamorphosed CM and CI carbonaceous chondrites could be from the breakup of the same earth-crossing asteroid. 36Th Lunar & Planetary Science Conference. (abstract #2084).